FINAL REPORT AFOSR-91-0160

INVESTIGATION OF FLAME DRIVING AND FLOW TURNING IN AXIAL SOLID ROCKET INSTABILITIES

Authors:

Ben T. Zinn, Brady R. Daniel, Lawrence M. Matta

School of Aerospace Engineering

Georgia Institute of Technology

Atlanta, GA 30332

31 August 1993

Final Report for Period 1 March 1991 - 30 June 1993

Approved for public release;

Distribution unlimited.

Prepared for:

AIR FORCE OFFICE OF SCIENTIFIC RESEARCH

Aerospace Sciences Directorate

Bolling Air Force Base

SECURITY CLASSIFICATION OF THIS PAGE (U)

REPORT DOCUMENTATION PAGE

Form Approved OMB No. 0704-0188

1a. REPORT SECURITY CLASSIFICATION Unclassified	1b. RESTRICTIVE MARKINGS
2a. SECURITY CLASSIFICATION AUTHORITY	3. DISTRIBUTION/AVAILABILITY OF REPORT approved for public release; Distribution unlimited
2b. DECLASSIFICATION/DOWNGRADING SCHEDULE	
4. PERFORMING ORGANIZATION REPORT NUMBER(S)	5. MONITORING ORGANIZATION REPORT NUMBER(S)
6a. NAME OF PERFORMING ORGANIZATION Georgia Institute of Technology School of Aerospace Engineering 6b. OFFICE SYMBOL (If applicable)	7a. NAME OF MONITORING ORGANIZATION Air Force Office of Scientific Research
6c. ADDRESS (City, State, and ZIP Code) Atlanta, Georgia 30332-0150	7b. ADDRESS (City, State, and ZIP Code) Same as 8c.
8a. NAME OF FUNDING/SPONSORING ORGANIZATION AFOSR 8b. OFFICE SYMBOL (If applicable) NA	9. PROCUREMENT INSTRUMENT IDENTIFICATION NUMBER AFOSR-91-0160
8c. ADDRESS (City, State, and ZIP Code) AFOSR NA 110 DUNCAN AVE SUITE B115 BOLLING AFB DC 20332-0001	10. SOURCE OF FUNDING NUMBERS PROGRAM ELEMENT NO. 61102F PROJECT NO. 2308 TASK NO. A5 WORK UNIT ACCESSION NO.

11. TITLE (Include Security Classification) "INVESTIGATION OF FLAME DRIVING AND FLOW TURNING IN AXIAL SOLID ROCKET INSTABILITIES" (U)

12. PERSONAL AUTHOR(S)
B. T. Zinn, B. R. Daniel and L. M. Matta

13a. TYPE OF REPORT	13b. TIME COVERED	14. DATE OF REPORT (Year, Month, Day)	15. PAGE COUNT
Final Report	FROM 910301 TO 930630	930831	77

16. SUPPLEMENTARY NOTATION

17. COSATI CODES			18. SUBJECT TERMS (Continue on reverse if necessary and identify by block number)
FIELD	GROUP	SUB-GROUP	Solid Propellant Rocket, Combustin Acoustics, Longitudinal Instability, Flow Turning Loss

19. ABSTRACT (Continue on reverse if necessary and identify by block number)

(SEE REVERSE FOR ABSTRACT)

20 DISTRIBUTION/AVAILABILITY OF ABSTRACT ☒ UNCLASSIFIED/UNLIMITED ☒ SAME AS RPT. ☐ DTIC USERS	21 ABSTRACT SECURITY CLASSIFICATION Unclassified
22a. NAME OF RESPONSIBLE INDIVIDUAL Dr. Mitat Birkan	22b. TELEPHONE (Include Area Code) (202) 767-4938 22c. OFFICE SYMBOL NA

DD Form 1473, JUN 86 *Previous editions are obsolete.*

SECURITY CLASSIFICATION OF THIS PAGE
Unclassified

ABSTRACT

An understanding of the processes responsible for driving and damping acoustic oscillations in solid rocket motors is necessary for developing practical design methods that eliminate or reduce the occurrence combustion instabilities. While state of the art solid rocket stability prediction methods generally account for the flow turning loss, the magnitude and characteristics of this loss have never been fully investigated. This report describes results of an investigation of the role of the flow turning loss in the stability of solid rockets and its dependence upon motor design and operating parameters. A one dimensional acoustic stability equation that verifies that the flow turning loss term is appropriately included in the one dimensional stability formulation was derived for a chamber with a constant mean temperature and pressure by an approach independent from that of Culick. This study was extended provided the background and expressions needed to guide an experimental study of the flow turning loss in the presence of mean temperature and density gradients. This allows the study of combustion systems in which mean temperature gradients and heat losses are significant. The relevant conservation equations were solved numerically for the experimental configuration in order to predict the behavior of the flow turning loss and to assist in the analysis of experimental results. Experiments performed, with and without combustion, showed that the flow turning loss strongly depends upon the propellant burning rate and the location of the flow turning region relative to the standing pressure wave. While the stability equation for flows with temperature gradients differs from the corresponding equation for cold flows, the measured behavior of the flow turning loss term was qualitatively similar in experiments with and without combustion.

INTRODUCTION

The objective of this research program was to develop a better understanding of the flow turning loss and other processes that contribute to the driving and damping of axial instabilities in solid rocket motors. This understanding is necessary for the development of dependable methods for designing motors that do not exhibit such instabilities.

The occurrence of combustion instabilities is determined by the relative magnitudes of the driving and damping mechanisms within the combustor that add and remove energy from the oscillations, respectively. If the acoustic energy gains outweigh the losses, small disturbances amplify to levels that can adversely affect guidance, thrust history, and the structural integrity of the motor[1-4]. Because of the high energy densities and low losses observed in most combustors designed for use in propulsion systems, the possibility of encountering instability is high. Combustion instability is a common problem in solid propellant rocket motors[5] as well as in other types of combustion systems. Since combustion instability can lead to system and/or mission failure, the development of reliable methods for predicting the stability of solid propellant rocket motors has been a long standing goal of the propulsion community.

In order to eliminate or reduce the severity of acoustic oscillations resulting from combustion instabilities in solid rocket motors, the mechanisms by which energy is added to and removed from these oscillations must be identified and understood. The interaction of the solid propellant combustion process with the acoustic oscillations in the combustor is generally accepted as the source of the energy necessary to initiate and maintain the instability. On the other hand, processes such as energy transmitted (out of the motor) through the choked nozzle, viscous dissipation, and flow turning tend to remove energy from the oscillations and, thus, stabilize the motor. While viscous damping is generally neglected in stability analysis, and much is

known about the processes of nozzle damping and combustion driving, relatively little is known about the flow turning loss.

The velocity of combustion products leaving the burning solid propellant is generally radial, as shown in Fig. 1. As these gases move away from the propellant and are entrained in the core flow, they are turned from the radial direction to axial. During this turning process, the combustion products acquire axial acoustic energy from the core flow oscillations. This phenomenon was first discussed by Culick[6-10] who argued that since the combustion products entering the core flow acquire acoustic energy from the existing axial acoustic core flow oscillations, the axial acoustic field experiences a loss of acoustic energy, which tends to stabilize the system.

The flow turning phenomenon has been studied experimentally by Hersch[11,12] and Chen[13] and analytically by Baum[14,15] and Hegde et al[16-18]. In these investigations, the behavior of acoustic waves in a channel in which the solid propellant combustion process was simulated by mass addition through a side wall was investigated. Hersch[11,12] used pressure measurements upstream and downstream of a region of wall injection to determine the influence of flow turning upon induced pressure oscillations. This study concluded that mass addition through the side wall resulted in damping of the axial acoustic field. The magnitude of the flow turning loss was determined to depend upon the frequency of oscillation, and was not linearly dependent upon the injection rate. These conclusions are inconsistent with the behavior of the flow turning loss as predicted by Culick[6-10]. The method used in this study determines the overall energy loss due to the injection, but cannot isolate the flow turning loss term as identified by Culick from other effects of the same order of magnitude as the flow turning loss that were present in the experiment. Chen[13] measured the acoustic intensity flux through the boundaries of a control volume in the flow turning region to determine the damping due to flow turning. This experimental method also cannot isolate the flow turning loss from other effects of the order of

similar order that are coupled with it. Baum's[14,15] computational studies show that the flow field near the wall is extremely complex, involving interactions between a multitude of vortical structures and energy exchange between the mean flow and the oscillations. Hegde[16-18] used a linear analysis and hot wire measurements to determine the acoustic characteristics and losses of a duct containing a standing axial acoustic wave and mass addition through the side wall. This investigation tested the validity of a linear stability model similar to those currently used to predict solid propellant rocket stability and performance, and in contrast to Baum's results, Hegde's studies suggest that a linear model, similar to those currently used to predict the stability of solid propellant rocket motors, may be adequately describe the important features of the flow turning loss.

The following questions were addressed in this study:

1. Is the flow turning loss properly included in currently used solid propellant rocket motor stability prediction programs?

2. What is the best approach for measuring the flow turning loss?

3. How does the flow turning loss depend upon the wall injection velocity, the axial core flow velocity, the frequency, and the location of the flow turning region relative to the standing pressure wave?

In the following section, the accomplishments of the research performed under the current program are discussed. First, the theoretical investigation of the flow turning loss, in which the basis for the experimental approach was developed, is described. Second, a simple computational model used to study the behavior of the flow turning loss and to assist in the interpretation of experimental results is discussed. Finally, the results of the experimental study are presented.

RESEARCH ACCOMPLISHMENTS

1) Theoretical Investigation

A theoretical investigation of the flow turning loss was performed in order to determine whether the flow turning loss is accurately included in state of the art stability prediction methods and to develop a practical method for measuring it. First, in order to verify the existence and mathematical form of the flow turning loss as defined by Culick[6], a one-dimensional acoustic stability equation was derived using an energy balance approach similar to that used by Cantrell and Hart[19] and later by Flandro[20] with the inclusion of flow rotation effects. The development of the stability equation begins with consideration of the energy equation accurate to second order in acoustic perturbations and first order in Mach number. A useful expression is then found containing products of only first order quantities by using the mass and momentum equations. The resulting stability equation is similar to that originally derived by Culick using a different theoretical approach. The stability equation for a two dimensional rectangular volume of length L and height H can be written as

$$2\alpha E^2 = -\left\langle \left[p_1 u_1 + \frac{p_1^2 u_0}{\rho_0 \bar{a}_0^2} + \rho_0 u_0 u_1^2 \right]_0^L \right\rangle_{t,y} - \left\langle \frac{1}{H} \int_0^L \left(\langle p_1 \rangle_y \left[\frac{m_{b1}}{\rho_0} \right]_0^H \right.\right.$$

$$\left.\left. + \langle u_1 \rangle_y [m_{b1} u_0]_0^H + \langle u_1 \rangle_y [m_{b0} u_1]_0^H - \langle u_1^2 \rangle_y [m_{b0}]_0^H \right) dx \right\rangle_t \qquad (1)$$

where α is the acoustic growth rate constant, u and v represent the velocity components in the axial and transverse directions respectively, and m_b is the mass flux at the wall. A numerical subscript represents the order of perturbation of the subscripted term (e.g., p_1 is the first order

pressure perturbation). Angle brackets, < >, represent an average over the subscript variable (e.g., $\langle\ \rangle_t$ represents a time average). E^2 is a term with units of energy given by

$$E^2 = \int_0^L \left\langle \frac{p_1^2}{2\rho_0 \bar{a}_0^2} + \frac{p_1 u_0 u_1}{\bar{a}_0^2} + \frac{\rho_0 u_1^2}{2} \right\rangle_{t,y} dx \tag{2}$$

Flandro[20] states that the inclusion of the second term in Eq. 2 is somewhat controversial, and demonstrates that this term is correctly placed and does not lead to results that are inconsistent with solutions of the linear problem carried out by other means.

The organization of the terms of Eq. 1 was performed in a way that facilitates a comparison with Culick's result. Culick[6], states "the combination [of terms] can be written in many equivalent ways; it is by no means obvious at this point which is most suitable". Culick argues that his chosen manner of combining the terms aids interpretation and incorporation into the three-dimensional problem. The term identified by Culick as "mean flow/acoustic surface interactions", later to become known as flow turning term, in Eq. 1 is

$$\text{FLOW TURNING LOSS} = \left\langle \frac{1}{H} \int_0^L \left\langle u_1^2 \right\rangle_y \left[m_{b0} \right]_0^H dx \right\rangle_t \tag{3}$$

Inspection of Eq. 3 shows that it will always be negative in a rocket motor, where mass enters through the burning surfaces. For such a configuration, this term tends to reduce α, thereby tending to stabilize the system. On the other hand, if mass exits the system through a side wall (such as through a T-burner nozzle), the term is positive, which increases α and destabilizes the system.

This analysis confirmed that the flow turning loss term is appropriately included in the one dimensional acoustic stability equation. The analysis also confirmed Van Moorhem's[21] conclusion

that the flow turning loss is not absent from the three dimensional analysis as suggested by Culick[7], but that the "classical flow turning" term can only be isolated after cross sectional averaging. Tracing the origin of the flow turning loss term backwards through the derivation shows that it originates in a rotation term of the axial momentum equation. The flow turning loss is implicitly included in any multi-dimensional analysis that does not impose irrotationality.

The one dimensional stability equation shown in Eq. 1 was derived by expanding the governing equations in terms of first and second order quantities. While such a procedure is theoretically sound, it is difficult to correlate first and second order quantities with measured experimental data. Therefore, a new theoretical approach, detailed in Ref. 22, has been developed which is more useful for the experimental determination of the flow turning loss. This approach starts with the equations of mass and axial momentum conservation in which each of the dependent variables is expressed in terms of a time averaged and a fluctuating component. For example, the pressure is expressed as $p = \bar{p} + p'$, where $\bar{p}$ is the time average of the measured pressure p.

The expression obtained by this method for the complex growth rate constant of the oscillations is

$$2\alpha E_m^2 = -\left\langle \left[p'u' + \frac{p'^2 \bar{u}}{\bar{\rho}\bar{a}^2} + \bar{\rho}\bar{u}u'^2 \right]_0^L \right\rangle_{t,y} - \left\langle \frac{1}{H}\int_0^L \left(\langle p' \rangle_y \left[\frac{m'_b}{\bar{\rho}} \right]_0^H \right. \right.$$

$$\left. \left. + \langle u' \rangle_y \left[m'_b \bar{u} \right]_0^H + \langle u' \rangle_y \left[\bar{m}_b u' \right]_0^H - \langle u'^2 \rangle_y \left[\bar{m}_b \right]_0^H \right) dx \right\rangle_t \qquad (4)$$

Comparison of Eqs. 1 and 4 reveals that the form of the equations is identical. However, the quantities involved in these equations are defined differently. Equation 3 lends itself more

rigorously to the verification of experimental results due to the way in which the terms have been defined.

In the above developments, the flow was assumed isentropic to facilitate the use of the energy balance approach based upon the Cantrell and Hart analysis. The result of this assumption was that Eq. 4 is limited to flows with uniform mean temperature and density. The above results cannot be used to analyze combustion systems in which mean temperature gradients and heat losses may be significant. In order to determine the effects of temperature gradients upon the acoustic stability and the flow turning loss term, an investigation of the non-isentropic equations was performed.

In this analysis, a stability equation that accounts for the mean temperature and density gradients that appear in the hot flow experimental studies was developed from the conservation equations for mass, axial momentum, and energy:

$$\frac{\partial \rho}{\partial t} + \frac{\partial}{\partial x}(\rho u) + \frac{\partial}{\partial y}(\rho v) = 0 \tag{5}$$

$$\rho \frac{\partial u}{\partial t} + \rho u \frac{\partial u}{\partial x} + \rho v \frac{\partial u}{\partial y} + \frac{\partial p}{\partial x} = 0 \tag{6}$$

$$P\left(\frac{\partial s}{\partial t} + u\frac{\partial s}{\partial x} + v\frac{\partial s}{\partial y}\right) = R\dot{Q} \tag{7}$$

where s is the specific entropy, R is the gas constant and $\dot{Q}$ is the rate of heat addition per volume. The energy equation was not used explicitly in the previous development. It was implicitly included in the isentropic relations. These equations were used together with the perfect gas equation of state,

$$p = \rho RT \tag{8}$$

where T is the temperature. In the analysis, it was assumed that $\dot{Q}' = 0$ (i.e., the unsteady heat addition or loss within the volume was neglected). The development, which is similar to the analysis used in the previous section, is detailed in Ref. 23. The resulting acoustic stability equation is:

$$2\alpha E_M^2 = -\left\langle \left[p'u' + \bar{\rho}\bar{u}u'^2 \right]_0^L \right\rangle_{t,y} - \int_0^L \left\langle \frac{\bar{u}p'}{\bar{\rho}\bar{a}^2}\left(\frac{\partial p'}{\partial x}\right) + \frac{\bar{u}\rho'}{\bar{\rho}}\left(\frac{\partial p'}{\partial x}\right) + \frac{p'^2}{\bar{p}}\left(\frac{\partial \bar{u}}{\partial x}\right) \right\rangle_{y,t} dx$$

$$-\left\langle \frac{1}{H}\int_0^L p'\left[v'\right]_0^H + \frac{p'^2}{\bar{p}}\left[\bar{v}\right]_0^H + \left\langle \bar{\rho}u' \right\rangle_y \left[\bar{u}v'\right]_0^H + \left\langle \bar{\rho}u' \right\rangle_y \left[u'\bar{v}\right]_0^H \right.$$

$$\left. -\left\langle \bar{\rho}u'^2 \right\rangle_y \left[\bar{v}\right]_0^H + \left\langle \bar{u}u'v' \right\rangle_y \left[\bar{\rho}\right]_0^H \right] dx \Bigg\rangle_t \tag{9}$$

where

$$E_M^2 = \int_0^L \left\langle \frac{p'^2}{2\bar{\rho}\bar{a}^2} + \rho'\bar{u}u' + \frac{\bar{\rho}u'^2}{2} \right\rangle_{t,y} dx \tag{10}$$

The most important differences to note between Eq. 9 and Eq. 4 is that $\bar{\rho}$ is not constant and $a^2 \neq \frac{p'}{\rho'}$ in Eq. 9. The term

$$\left\langle \frac{1}{H}\int_0^L \left\langle \bar{\rho}u'^2 \right\rangle_y \left[\bar{v}\right]_0^H dx \right\rangle_t$$

is identified as the flow turning term in this version of the stability equation, and compares to the flow turning term of the constant density stability equation, shown in Eq. 3.

The term

$$\left\langle \frac{1}{H}\int_0^L \langle \bar{u}u'v' \rangle_y [\bar{\rho}]_0^H dx \right\rangle_t$$

which appears in Eq. 9, does not appear at all in Eq. 4 because $[\bar{\rho}]_0^H = 0$ in the previous analysis. Comparison of the equations shows that the term

$$\int_0^L \left\langle \frac{\bar{u}p'}{\bar{\rho}\bar{a}^2}\left(\frac{\partial p'}{\partial x}\right) + \frac{\bar{u}\rho'}{\bar{\rho}}\left(\frac{\partial p'}{\partial x}\right) + \frac{p'^2}{\bar{p}}\left(\frac{\partial \bar{u}}{\partial x}\right) \right\rangle_{y,t} dx$$

in the stability equation that accounts for temperature gradients, Eq. 9, relates to the term

$$\left\langle \left[\frac{p'^2 \bar{u}}{\bar{\rho}\bar{a}^2} \right]_0^L \right\rangle_{t,y}$$

in Eq. 4. The term from Eq. 4 represents fluxes through the axial boundaries of the control volume, while the term from Eq. 9 cannot be reduced to a surface flux term, and represents effects that occur inside the volume. This difference is due to the inclusion of density gradients in Eq. 9, and suggests that the interaction of axial acoustics with axial density gradients in the presence of a mean flow may drive or damp the acoustics.

2) Numerical Simulation

In an effort to determine the behavior of the various terms involved in the derived acoustic stability equation, Eq. 3, the experimental setup used in the flow turning investigation was modeled numerically. Figure 2 shows the simulated setup in which the length L, the height H, the distance from the head end to the burner $L1$, and the distance from the head end to the end of the burner $L2$ are characteristic lengths of the experimental setup. This simulation involved the derivation and numerical solution of the mass and momentum conservation equations that describe the experimental setup and the test conditions. For this analysis, the flow was assumed to be isentropic with perturbations that are harmonic in time. The two dimensional forms of the equations were averaged over the cross-section of the duct and then integrated along the axis of the experimental setup. The solutions were then substituted into the developed acoustic stability equation to determine the values of the terms that affect the stability of the system and to determine whether the numerical solution satisfies Eq. 4.

It should be noted that the numerical simulation models the experimental setup and not an unstable solid propellant rocket motor. Several important differences exist between the behaviors of the experimental setup and an actual solid rocket motor that affect the nature of the simulation. The most important difference is that the experiment is an externally driven system, while an unstable rocket motor is a self driving system. One result is that the experimental system is always neutrally stable; i.e., the oscillations neither amplify nor decay in time. This means that while the various terms of the acoustic stability equation may change for different configurations, the resulting growth rate constant α must equal 0 for the experiment. On the other hand, the growth rate for the oscillations in a rocket motor is determined by the sum of the terms in Eq. 4. Another difference is that the frequency of oscillation in the experimental setup is known; i.e., chosen by the experimenter, whereas the frequency of oscillation in an unstable rocket motor is determined by relevant conditions (e.g., the geometry and temperature) and is not easily predicted. With this in mind, the ability of the numerical simulation to satisfy the derived stability

equation is determined by summing the calculated values of the terms on the right hand side of Eq. 4. The sum of the terms, and thus the growth rate α, should equal 0. Calculations were carried out for a number of different experimental configurations, and in all cases, excellent agreement between the results of the numerical simulation and the developed stability equation was observed.

Results of a simulation for a simple experimental configuration are shown in Figs. 3 and 4. For this example, the admittances of the upstream injector, the top and bottom walls, and the burner surface are assumed to be zero in order to simplify the calculations. The conditions for the simulations have been set as follows: 1) the mean pressure is atmospheric, 2) the amplitude of the pressure oscillation at the injector face is 200 Pa, 3) the burner is 10 cm long and is located 70 cm downstream of the injector, and 4) the mean Mach number of the flow through the burner is 0.004, which simulates the Mach number of the flow at the multi-diffusion flame burner surface for a typical cold flow experiment. Figure 3 describes the axial variations of the amplitude and phase of the acoustic pressure oscillation in the experimental setup. The location of the burner is shown in the figure. It is seen from the figure that the effect of mass addition upon the pressure is small for the investigated Mach number. The axial variations in of the relevant terms of the acoustic stability equation, Eq. 4, are described in Fig. 4. The sum of these terms, which is proportional to α, is also shown (term 6 in the figure), and is equal to 0 at all locations, which is in agreement with the theory and the discussion in the previous paragraph. It should be noted that for this burner surface Mach number, the calculated flow turning loss is small. This is due to the low Mach number and the short burner length (the flow turning loss accumulates over length), and does not suggest that the flow turning loss is insignificant in a solid rocket motor. Figure 4 also shows that the terms of Eq. 4 which are of first order in Mach number tend to be of similar magnitude. As a result, previous experimental studies[13] could not effectively measure the flow turning loss because the effects of all relevant terms were not accounted for.

The effects of several parameters upon the magnitude of the flow turning loss were studied using the numerical simulation procedure. One such parameter was the location of the simulated burner relative to the standing acoustic wave. Figure 5 indicates that the flow turning loss is dependent upon the relative location of the side wall mass injection. The flow turning loss is greatest when the burner is located at an axial acoustic velocity maximum, and is least when the burner is at a velocity minimum. Another investigated parameter was the mean core flow Mach number. A series of simulations in which the mean core flow Mach number M_C was varied from $M_C = 0.0$ to $M_C = 0.1$ demonstrated that the magnitude of the flow turning loss is independent of the core flow velocity over the investigated range. Figure 6 shows that while the magnitude of some terms change (specifically, the mean flow convection terms), the flow turning term remains unchanged in all cases. Results of the third parameter studied, the burner injection Mach number M_B, are displayed in Fig. 7. This investigation showed that the magnitude of the flow turning loss varies linearly with the injection Mach number.

The conditions used for the initial numerical simulations were idealized in order to simplify the interpretation of the results. The actual conditions encountered in the experimental investigation are rather complex, and difficult to approximate in a numerical simulation. Therefore, the numerical simulation was modified to use experimentally determined (i.e., measured) boundary conditions. This version of the code is used to aid in interpretation of experimental results.

The simulations involving experimentally determined boundary conditions require measured values of the mean axial velocity component at the initial axial boundary of the control volume as shown in Fig. 8, the amplitude and phase of the axial acoustic velocity component at both axial boundaries, as well as the vertical velocity component and the amplitude and phase of the vertical acoustic velocity along the top and bottom boundaries. A shooting method is then used to determine the acoustic velocity and pressure solutions which minimize the errors at the axial

boundaries in a least squares sense. These values of velocity and pressure are then used along with Eq. 3 to predict values of the various terms in the acoustic stability equation. The results of this type of simulation and the comparison with experimental results are discussed in the next section.

3) Experimental Study

The experimental setup used in this study is shown schematically in Fig. 9. Details of the experimental setup are given if Ref. 24. The setup is designed to simulate flow phenomena near the walls of a solid propellant rocket experiencing an axial acoustic instability. In the first phase of the study, cold flow experiments were performed to determine the validity of the "flow turning" loss and its effect upon the acoustic stability. In the second phase of the experimental study, a multi-diffusion flame burner (shown schematically in Fig. 10) was used to better simulate actual motor conditions and to determine the influence of temperature gradients upon the flow turning loss and upon other factors relevant to the stability of rocket motors.

a) Cold Flow Studies

In the cold flow investigation, the flow turning loss and α_{FTL} were determined by measuring the two components of the mean and acoustic velocities and the acoustic pressure and then substituting the measured values into Eq. 4. The term α_{FTL} describes the contribution of the flow turning loss to the growth rate constant α of the investigated region, and is defined as:

$$\alpha_{FTL} = \left\langle \frac{1}{H} \int_0^L \left\langle u_1^2 \right\rangle_y \left[m_{b0} \right]_0^H dx \right\rangle_t \Big/ 2E_M^2 \qquad (11)$$

A number of experiments were performed for various conditions to determine the effects of these conditions upon the flow turning loss. Several hours were required to acquire the necessary

velocity and pressure data for each configuration. Due to the slow data acquisition and the sensitivity of the flow field to experimental conditions, only a small number of data per configuration (generally 3) were collected. To compensate, a large number of experimental runs were performed, and trends were determined by comparing a number of results.

The results displayed in Fig. 11 shows the effect of the burner injection velocity upon α_{FTL} in the investigated region. The results were obtained in a test conducted with a frequency of 550 Hz., a mean core flow velocity of 0.4 m/s, and injection at a pressure node. The measured α_{FTL} varies linearly with the mean burner injection velocity.

Figure 12 shows the dependence of α_{FTL} in the investigated region upon the mean core flow velocity. This test was conducted with a frequency of 550 Hz., a burner injection velocity of 0.156 m/s, and the burner located at a pressure node. The measured α_{FTL} increase with the mean core flow velocity. The trend of this data and the results of other tests (because a conclusion cannot be drawn from three data points) shows that α_{FTL} appears to approach a limit value as the core velocity increases. This is due to incomplete turning of the flow inside the investigated region. In the experimental study, the investigated control volume does not extend from the burner surface to the top wall. Inspection of the mean velocity profile shown in Fig. 13 reveals that the flow at the top of the investigated control volume is not fully turned into the axial direction. As the core flow Mach number increases, flow turning is completed to a higher degree within the investigated control volume. Therefore, it is expected that as the core flow Mach number increases, the flow turning loss will also increase, which is consistent with the trend of the measured data.

The effect of varying the amplitude of the excited standing wave upon α_{FTL} is displayed in Fig. 14. The results are from an experiment in which the mean core flow velocity was 1.45 m/s, the mean burner injection velocity was 0.62 m/s, the frequency was 550 Hz., and the injection

occurred at an acoustic pressure antinode. The pressure amplitudes were normalized with respect to the maximum measured amplitude. The figure shows that α_{FTL} is independent of the amplitude of oscillation, which is expected in a linear analysis.

The dependence of α_{FTL} upon the location of the flow turning region with respect to the standing acoustic wave is shown in Fig. 15. These data were obtained in experiments with a mean core velocity of 2.86 m/s, a mean burner injection velocity of 1.34 m/s, and a frequency of 550 Hz. The measured α_{FTL} was maximum when the flow turning occurred at an acoustic pressure node, and minimum when the flow turning region was located at a pressure antinode.

b) Comparison of Experimental Data to Calculations

As discussed above, the numerical scheme was modified to use measured boundary conditions to aid in the interpretation of the measured data. Measured and calculated values of the axial acoustic velocity for an experimental test are shown in Fig. 16. The agreement between the measured and calculated velocity values is excellent. Figure 17 shows comparisons between measured and calculated acoustic pressures and measured and calculated phase angle between the pressure and velocity oscillations. A good qualitative agreement between the calculated and measured results is observed, but the error in the predicted phase values is large. The calculated and measured values of the flow turning loss for this test configuration are shown in Fig. 18. An excellent agreement is observed between the measured and calculated values. Note that, for the experimental configuration whose results are shown in this section, the value of the flow turning loss term was negative, indicating a gain of acoustic energy. This is the case because of the nature of the flow in the investigated control volume. The flow injected through the burner is turned into the axial direction, but at the same time, the core flow entering the control volume from upstream is being turned upward. For some experimental configurations, the flow turning loss due to the turning of the injected flow is smaller than the 'flow turning gain' due to the turning

of the core flow. This flow turning gain effect is observed only because of the choice of control volumes; in a volume extending from wall to wall (e.g., in a solid rocket motor) flow turning will always result in a loss of acoustic energy.

c) Hot Flow Studies

The results of an experimental study of the effects of mean temperature gradients upon the flow turning loss and other factors relevant to the stability of rocket motors are discussed in this section. Combustion is present in these hot flow studies, but the combustion region itself is kept external to the investigated region, as described in Fig. 19. The driving and damping effects of the combustion process have been studied previously in this research program by Sankar[25] and Chen[13], and the inclusion of these mechanisms would serve to complicate the flow turning analysis by coupling additional terms in the stability analysis. The data acquired in the hot flow experiments was analyzed using the form of the stability equation shown in Eq. 9, which accounts for spatial variations in the mean density.

A large temperature difference exists between the core flow (which consists of room temperature air) and the flow of hot combustion products leaving the flat flame that is stabilized above the burner surface. This generates a line of maximum temperature gradient begins at the upstream edge of the burner and follows the turning of the injected flow, as illustrated in Fig. 20. The flow turning loss and α_{FTL} in the hot flow experiments were determined by measuring the two components of the mean and acoustic velocities, the mean density, and the acoustic pressure in the investigated region and then substituting the measured values into Eq. 9. Experiments were performed for various conditions to determine the effects upon the flow turning loss.

The results shown in Fig. 21 were obtained in a test conducted with a frequency of 580 Hz., a mean core mass flow rate of 3.63 g/s, and the burner located at a pressure node, and cold flow results from an experiment in which the core mass flow rate was the same, the burner was located

at a pressure node, and the frequency was reduced to 300 Hz. The frequency was reduced in the cold flow tests to preserve the wavelength of the pressure oscillation under the cold flow conditions. The linear dependence of α_{FTL} upon the burner mass flow rate agrees with the theory. Comparison of the hot and cold results shows that the overall flow turning loss is greater in the cold flow cases. This is somewhat misleading, however, because the geometry of the hot flow field is not the same as that of the cold flow field. While the mass flow rates are preserved between the two configurations, the velocity out of the burner surface is much higher in the hot flow case. The result of the flow differences is that the stream of hot combustion products leaving the burner turns more gradually as it moves away from the burner than the flow of injected cold flow air. A qualitative comparison can be made, however, between the behavior of α_{FTL} under hot and cold conditions to determine the effect of the presence of temperature gradients. Qualitatively, the results show that the effect of the wall injection velocity upon flow turning loss, as determined by α_{FTL}, is virtually unaffected by the presence of mean temperature and density gradients in the flow turning region. The theoretical analysis shows that some effect of the density gradient should be present, but the measurements suggest that the influence of the density gradient is small compared to the effect of the injected mass flow rate in the studied configuration. It is likely that the effect of the density gradients upon the flow turning loss in actual solid rocket motors will also be small, because mean density changes encountered in actual solid rocket motors are generally small fractions of the total density.

Figure 22 shows the dependence of α_{FTL} upon the mean core mass flow rate measured in tests conducted with a frequency of 580 Hz. and an injected mass flow rate of 2.26 g/s through the burner, which was located at a pressure node. The measured α_{FTL} increase with the mean core flow velocity and appears to approach a limit. This behavior results from incomplete flow turning in the investigated region, as was explained in the discussion of the cold flow results. The cold flow data is from an experiment in which the mass flow rate through the burner was the

same, the burner was located at a pressure node, and the frequency was reduced to 300 Hz (to preserve the wavelength). Qualitative comparison again shows little difference between the behavior of α_{FTL} in the hot and cold flow experiments.

The dependence of α_{FTL} upon the location of the flow turning region with respect to the standing acoustic wave is shown in Fig. 23. These data were obtained in hot and cold experiments with a mean core mass flow of 3.63 g/s, and a mean mass flow through the burner of 2.26 g/s. The measured α_{FTL} was maximum when the burner was located at an acoustic pressure node, and minimum when the burner was located at a pressure antinode. No influence of the density gradient upon the behavior of α_{FTL} is suggested by the theory in this case, because the position of the burner relative to the standing acoustic wave has no influence on the mean temperature distribution in the combustor.

The terms of the acoustic stability equation that are proportional to the mean Mach number (e.g., flow as turning loss term) measured in this study were found to be much smaller than the Mach number independent terms (i.e., the classical acoustic intensity terms) in the experimental setup. This is due to the large acoustic admittance of the burner, which absorbs a large fraction of the acoustic energy of the investigated control volume. This, however, is not typical of the conditions encountered in actual solid propellant rocket motors, in which the response of the propellant is much smaller than that of the burner used in this study. The Naval Weapons Center has been involved in a program to develop an increased understanding of combustion instability through which a database of motor and stability data is being collected[26-30]. Blomshield et al[30] test fired 23 motors in a number of configurations, measured the decay rate of induced oscillations, and compared the data to stability predictions made using the Standard Stability Prediction Program (SSP-1D)[31]. The stability analysis performed in the SSP module is based upon Culick's stability formulation. The results show that for the test motors, the flow turning loss is very important to the overall stability of the motor. Other calculations of the stability of

full scale motors[31] show that, unlike the laboratory combustor used in this study, the flow turning loss is often a determining factor in the stability of solid propellant rocket motors due to the relatively small acoustic response of solid propellant compared to the multi-diffusion flame burner used in this study.

d) Effect of Temperature Gradients Upon The Acoustic Intensity

In a study performed by Chen[13], a significant amount of acoustic energy was absorbed in a region above a side wall stabilized, flat diffusion flame, but no significant energy loss was observed under cold flow conditions. The greater damping in the presence of combustion suggested that some process, possibly due to the presence of mean temperature gradients, contributes to the dissipation of acoustic energy in the system. This result does not agree with analytical studies, which show that for low mean Mach numbers, the presence of a mean temperature gradient neither drives or damps acoustic energy.

An experimental study of Chen's result was performed. The oscillatory velocities and pressures were measured on the border of a control volume located above the burner surface as shown in Fig 24. These measurements were used to calculate the classical acoustic intensity flux, $\langle p' \vec{V}' \rangle_t$, entering and leaving the boundaries of a two dimensional control volume above the multi-diffusion flame burner. The control volume investigated for this study was a 6.8 x 2.24 cm^2 rectangle located at the center plane of the duct. Measurements of the oscillatory velocities and pressures in this study were carried out with the burner at various locations relative to the standing acoustic wave, with and without combustion. The acoustic oscillation was driven at 700 Hz..

The measured acoustic intensity fluxes were used to determine the influence of the location of injection relative to the standing acoustic wave upon the energy absorption in the control volume. Figure 25 compares the ratio of the total acoustic intensity flux out of the control

volume to the flux through the downstream boundary (the direction of the acoustic driving) for hot and cold flow cases. Figure 25 does not show substantially more energy absorption in hot flow cases than in cold flow, and does not show a definite dependence of the energy absorption upon the location of the burner in the acoustic field. An average error of one degree in the phase angle between the pressure and velocity can result in as much as a 5 percent error in the calculated energy loss. Within this range, there is no discernible difference between the energy absorption with and without combustion, which agrees with the theoretical results.

SUMMARY

An investigation of the processes that control the flow turning loss and its role in the damping of combustion instabilities in solid propellant rocket motors has been performed. Theoretical, experimental, and numerical approaches have been used to study the behavior of the flow turning loss in a laboratory combustor designed to simulate important features of a solid rocket motor experiencing axial instability.

Theoretical analysis performed in this study has confirmed that the flow turning loss term must be included in the one dimensional acoustic stability equation. The analysis also confirmed that the flow turning loss is not absent from multi-dimensional formulations, but that the term traditionally identified as the flow turning loss occurs as a consequence of averaging the equations over the cross section of the chamber. The spatial averaging process has a tendency to make the physical interpretation of terms somewhat difficult. Tracing the flow turning loss term backwards through the analysis has shown that it originates in the rotational terms of the conservation equations, and indeed, the term does not appear in analyses that do not account for rotation of the flow.

An acoustic stability equation that accounts for the presence of mean temperature and density gradients in the chamber has been developed. This equation is similar in form to the stability formulae developed under the previous analyses. An additional term appears in the stability equation that accounts for cross-duct temperature gradients.

An experimental study was conducted in a setup designed to simulate flow phenomena near the walls of a solid propellant rocket experiencing an axial acoustic instability. A cold flow investigation was performed, in which the flow turning loss and α_{FTL} were determined by measuring the two components of the mean and acoustic velocities and the acoustic pressure and then substituting the measured values into the acoustic stability equation. Experiments were

performed to determine the effects of various parameters upon the flow turning loss. The flow turning loss was shown to be linearly dependent upon the wall injection velocity, which relates to the burning rate of the propellant on the walls of a rocket motor. This result agrees with theoretical predictions. Measurements showed that the flow turning loss in the experimental setup increased towards a limiting value as the core flow velocity was increased. This does not agree with theoretical predictions, which indicate that the flow turning loss is independent of the core flow velocity. This discrepancy is due to incomplete turning of the injected flow in the investigated region, and that under the conditions encountered in an actual rocket motor, the flow turning loss will be independent of the core flow velocity. The flow turning loss has been shown to be independent of the amplitude of oscillation over the investigated range. Because terms of third order and higher in the energy equation have been neglected, this behavior cannot be extrapolated to large amplitude oscillations. This is of no real concern, however, because linear analysis is generally performed when the oscillations are small. Also, the study has shown that the flow turning loss is maximum and minimum when the side wall injection occurs at acoustic pressure nodes and antinodes, respectively.

The terms proportional to the mean Mach number (such as the flow turning loss term) measured in this analysis were found to be much smaller than the Mach number independent terms (the classical acoustic intensity terms) in the experimental setup. This is because the burner is acoustically 'soft' and absorbs a great deal of acoustic energy. The result is that the zeroeth order (Mach number independent) losses in the experimental setup are high. This is not necessarily the case in actual solid propellant rocket motors, where the propellant response is generally small and the Mach numbers are somewhat higher. In actual motors, the flow turning loss and other terms of similar order are often of the same magnitude as the propellant response terms.

In the hot flow study, the effects of mean temperature gradients upon the flow turning loss and other factors relevant to the stability of rocket motors were investigated. The data acquired

in the hot flow experiments were analyzed using the stability equation formulated to account for spatial variations in the mean temperature. Measurements show that the behavior of the flow turning loss in the experimental setup is not significantly affected by the presence of a mean temperature gradient.

In contrast to the results of the previous study, measurements did not show substantial differences in the amount of energy absorbed in hot flow cases to that absorbed in cold flow, and does not show a definite dependence of the energy absorption upon the location of the burner in the acoustic field. The current results show that there is no difference outside the range of experimental error between the amount of energy absorbed with and without combustion. Theory suggests that, when terms proportional to the mean velocity are neglected, the stability of a duct is not influenced by the presence of mean temperature gradients, which agrees with the results of this study.

REFERENCES

1) McClure, F. T., Hart, R. W., and Cantrell, R. H., "Interaction Between Sound and Flow: Stability of T-Burners," *AIAA Journal*, Vol. 1, No. 3, March 1963.

2) Derr, R. L., Mathes, H. B., and Crump, J. E., "Application of Combustion Instability Research to Solid Rocket Motor Problems," *Proceedings of the 53rd Meeting of the NATO AGARD Propulsion and Energetics Panel*, Oslo, Norway, April 2-5, 1979.

3) Baum, J. D., "Acoustic Energy Exchange Through Flow Turning," AIAA Paper No. 87-0217, presented at the 25th Aerospace Sciences Meeting, Jan. 12-15, 1987, Reno, NV.

4) Sutton, G. P., *Rocket Propulsion Elements*, 5th Ed., pp. 310-312, John Wiley and Sons, Inc., 1986.

5) *Technical Panel on Solid Propellant Combustion: Scientific Papers, 1960-1963*, The Johns Hopkins University, Applied Physics Laboratory, Silver Spring, MD.

6) Culick, F. E. C., "The Stability of One Dimensional Motions in a Rocket Motor", *Combustion Science and Technology*, Vol. 7, 1973, pp. 165-175.

7) Culick, F. E. C., "Stability of Three-Dimensional Motions in a Combustion Chamber," *Combustion Science and Technology*, Vol. 10, 1975, pp. 109-124.

8) Culick, F. E. C., "Remarks on Entropy Production in the One Dimensional Approximation to Unsteady Flow in Combustion Chambers," *Combustion Science and Technology*, Vol. 15, 1977.

9) Culick, F. E. C., Magiawala, K., Wat, J., Awad, E., and Kubota, T., "Measurements of Energy Losses Associated with Interactions Between Acoustic Waves and Non-Uniform Steady Flow," AFRPL-TR-81-22, 1981.

10) Culick, F. E. C., "Combustion Instabilities in Propulsion Systems," presented at The Winter Annual Meeting of the Society of Mechanical Engineers, San Francisco, CA December 10-15, 1989.

11) Hersch, A. S., and Walker, B., "Experimental Investigation of Rocket Motor Flow Turning Losses," AIAA Paper No. 83-1267, June 1983.

12) Hersch, A. S., and Tso, J., "Flow Turning Losses in Solid Rocket Motors," AFAL-TR-095, March 1988.

13) Chen, T., *Driving of Axial Acoustic Fields By Sidewall Stabilized Diffusion Flames*, Ph.D. Thesis, Georgia Institute of Technology, July 1990.

14) Baum, J. D., and Levine, J. N., "Acoustic-Mean Flow Interaction," AFRPL-TR-86-065, January 1987.

15) Baum, J. D., "Numerical Investigation of Energy Exchange Mechanisms Between Mean and Acoustic Flow Fields in a Simulated Rocket Combustor," AIAA-90-2310, 26th Joint Propulsion Conference, Orlando, FL, 1990.

16) Hegde, U. G., Chen, F., and Zinn, B. T., "Investigation of the Acoustic Boundary Layer in Porous Walled Ducts With Flow," *AIAA Journal*, Vol. 24, No. 9, pp. 1474-1482, September 1986.

17) Hegde, U. G., and Zinn, B. T., "Rocket Motor Flow Turning Losses," *AIAA Journal*, Vol. 24, No. 8, pp. 1394-1396, August, 1986.

18) Hegde, U. G., and Zinn, B. T., "The Acoustic Boundary Layer in Porous Walled Ducts With a Reacting Flow," *Proceedings of the Twenty-First Symposium on Combustion*, August 1986.

19) Cantrell, R. H., and Hart, R. W., "Interactions Between Sound and Flow in Acoustic Cavities: Mass, Momentum, and Energy Considerations," *Journal of the Acoustic Society of America*, Vol. 36, No. 4, April 1964.

20) Flandro, G. A., "Energy Balance Analysis of Nonlinear Combustion Instability," Journal of Propulsion and Power, Vol. 1, May 1985.

21) Van Moorhem, W. K., "Theoretical Basis of the Flow Turning Effect in Combustion Stability," Final Report, AFOSR Grant No. 78-3654, March 1980.

22) L. M. Matta, B. T. Zinn, and B. R. Daniel, "Theoretical Investigation of Flow Turning Losses in an Experimental Setup Which Simulates Instabilities in Solid Propellant Rocket Motors", AIAA Paper No. 92-0780, AIAA 30th Aerospace Sciences Meeting, Reno, NV, Jan 6-9, 1992.

23) L. M. Matta and B. T. Zinn, "Theoretical Study Of Flow Turning Losses In The Presence Of Mean Temperature Gradients", to be presented at the AIAA 32th Aerospace Sciences Meeting, Reno, NV, 1994.

24) L. M. Matta and B. T. Zinn, "Investigation Of Flow Turning Loss In A Simulated Unstable Solid Propellant Rocket Motor", AIAA Paper No. 93-0115, AIAA 31st Aerospace Sciences Meeting, Reno, NV, Jan 11-14, 1993.

25) Sankar, S. V., *Investigation of Flame-Acoustic Wave Interaction During Axial Solid Rocket Instabilities*, Ph.D. Thesis, Georgia Institute of Technology, September 1987.

26) Blomshield, F.S., Crump, H.B., Mathes, H.B., Derr, R.L., and Beckstead, M.L., "TTCP Non-Linear Instability Collaborative Program - NWC Participation," 22nd JANNAF Combustion Meeting, 1985.

27) Clark, W.H., Crump, H.B., Mathes, H.B., and Beckstead, M.L., "Motor Test Data Comparisons With Laboratory Data and Stability Predictions," 24th JANNAF Combustion Meeting, 1987.

28) Clark, W.H., Crump, H.B., and Mathes, H.B., "Results of Tests for Non-Linear Stability of Full Scale Rocket Motors," 25th JANNAF Combustion Meeting, 1988.

29) Blomshield, F.S., Crump, H.B., Mathes, H.B., and Beckstead, M.L., "Stability Testing of Full Scale Tactical Motors," 27th JANNAF Combustion Meeting, 1990.

30) Blomshield, F.S., Crump, H.B., Mathes, H.B., and Beckstead, M.L., "Stability Testing of Full Scale Tactical Motors," AIAA Paper No. 91-1954, AIAA/SAE/ASME 27th Joint Propulsion Conference, 1991.

31) Nickerson, G. R., Culick, F. E. C., and Dang, A. L., "The Solid Rocket Motor Performance Computer Program (SPP), Version 6.0", Volume VI: Standard Stability Prediction Method for Solid Rocket Motors, AFAL-TR-87-078.

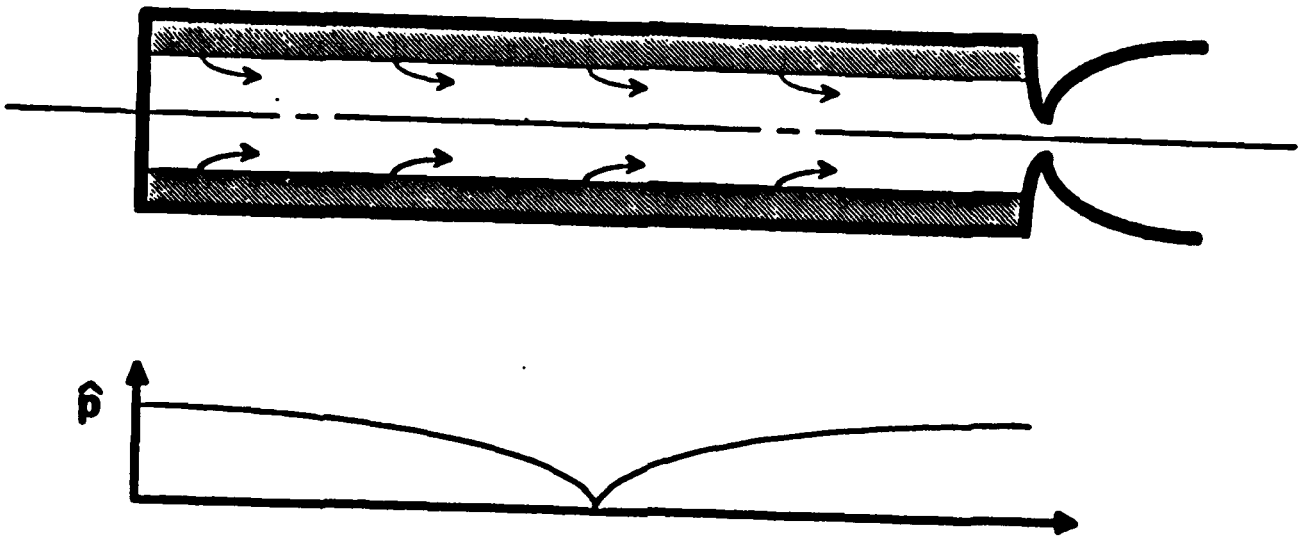

Figure 1. Schematic of a solid propellant rocket motor showing the flow of combustion products turning from radial to axial as they are entrained into the core flow and the pressure distribution characteristic of axial acoustic instability.

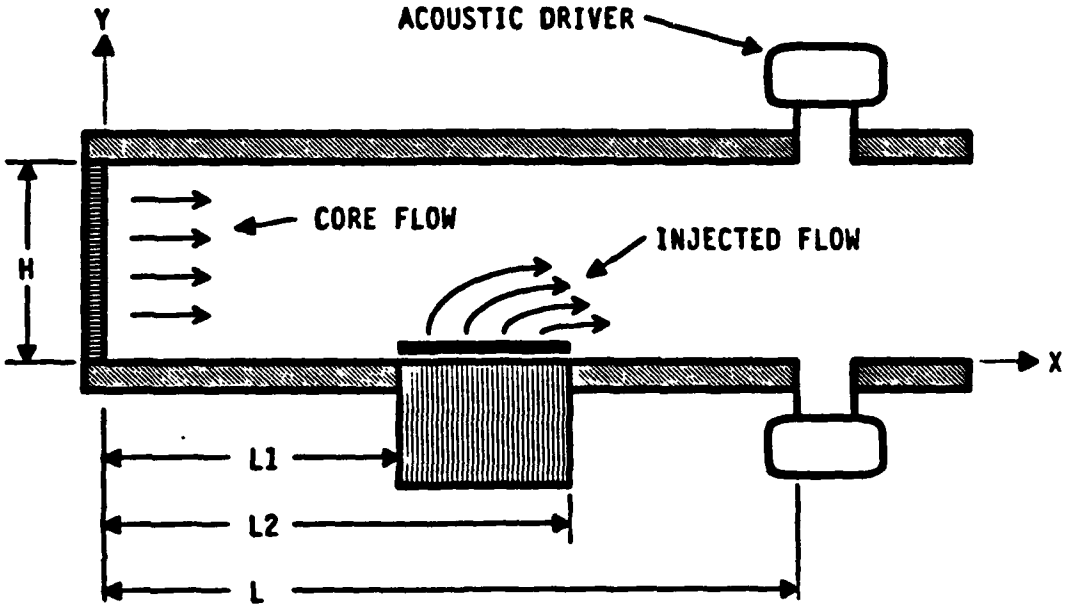

Figure 2. Schematic of the configuration used in the numerical simulation of the experimental setup.

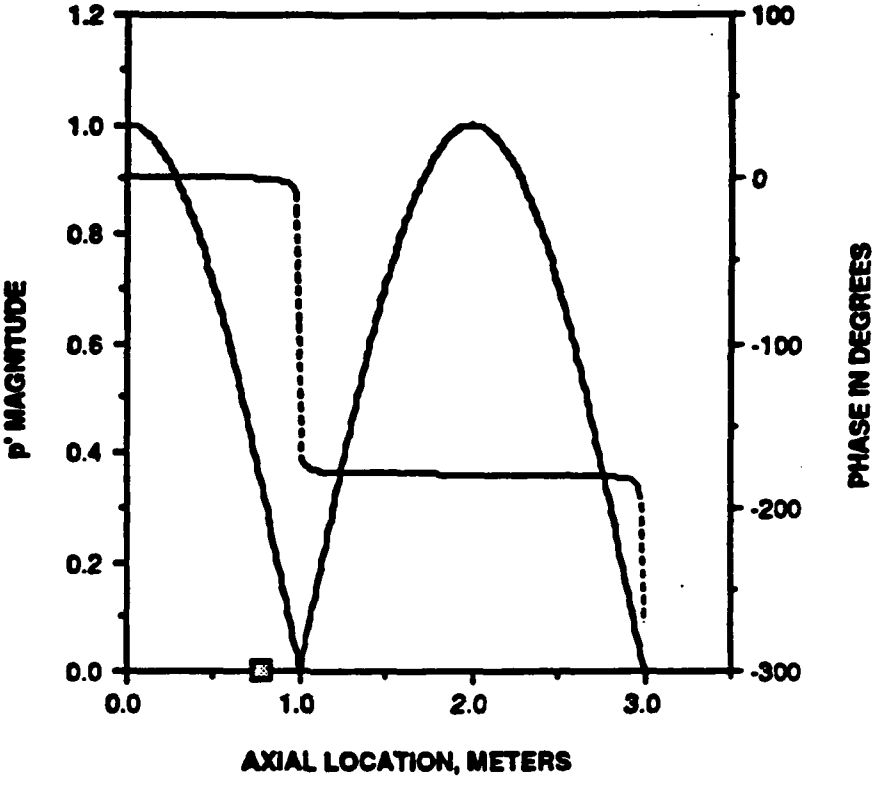

SOLID LINE - NORMALIZED AMPLITUDE OF p'
BROKEN LINE - PHASE OF ACOUSTIC PRESSURE p'

Figure 3. Numerically predicted amplitude and phase of the pressure oscillation with side injection near an acoustic pressure minimum.

TYPICAL NUMERICALLY PREDICTED DATA

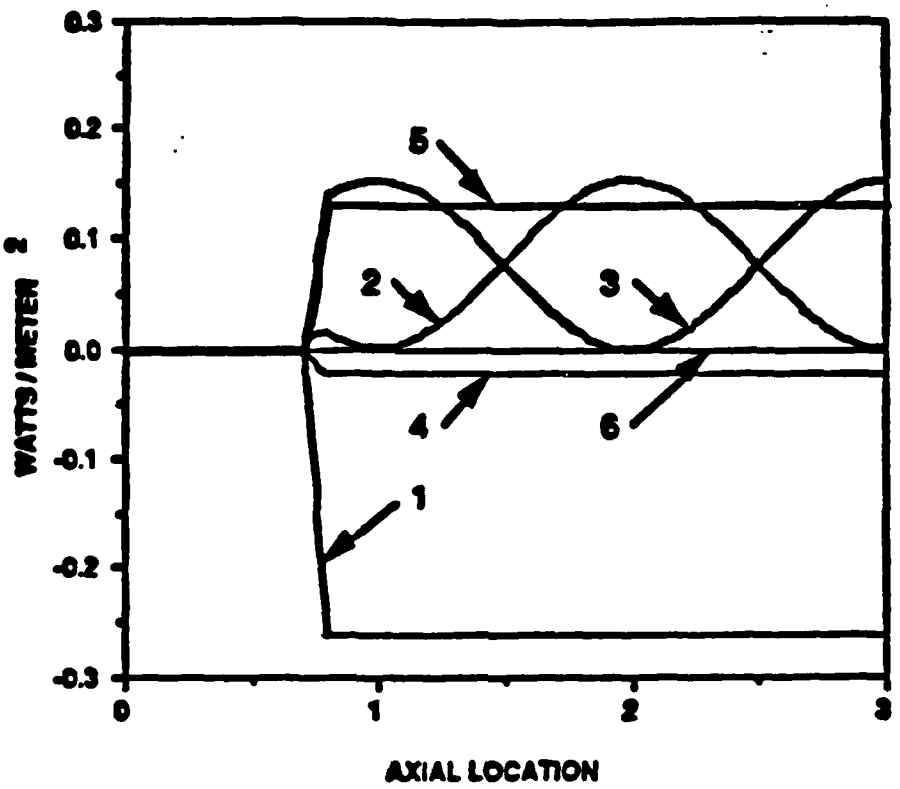

$$-2\alpha E_m^2 = \underbrace{\left\langle \left[p' u' + \frac{p'^2 \bar{u}}{\bar{\rho} \bar{a}^2} + \bar{\rho} \bar{u} u'^2 \right]_0^x \right\rangle_{t,y}}_{1,2,3} + \underbrace{\left\langle \frac{1}{H} \int_0^x \langle p' \rangle_y \left[\frac{m'_b}{\bar{\rho}} \right]_0^H dx \right\rangle_t}_{4}$$

$$\underbrace{-\left\langle \frac{1}{H} \int_0^x \langle u'^2 \rangle_y [\bar{m}_b]_0^H dx \right\rangle_t}_{5 = \text{THE FLOW TURNING LOSS}}$$

Figure 4. Numerical prediction of the relevant terms of the acoustic stability equation.

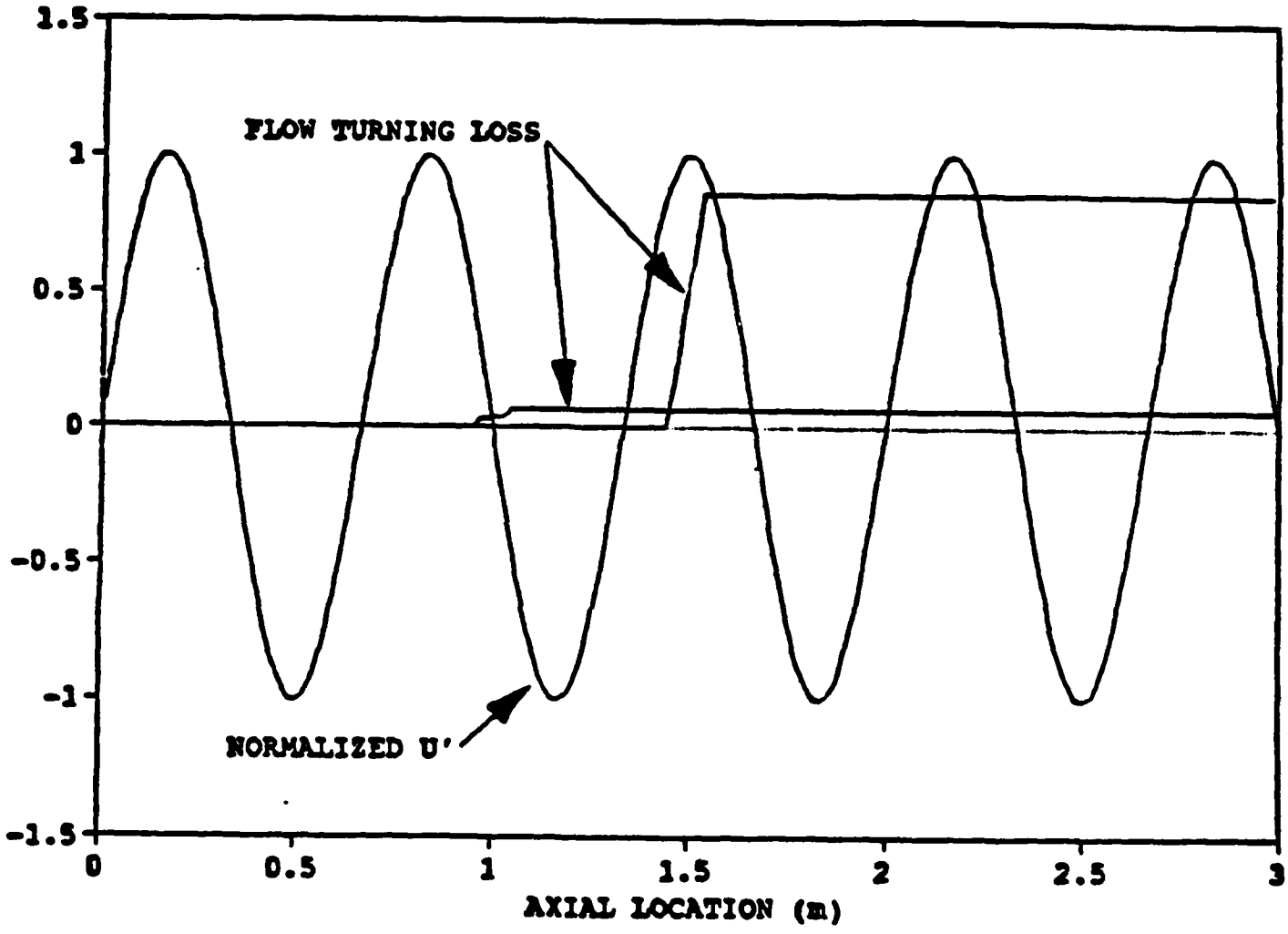

Figure 5. Predicted flow turning loss for injection at an acoustic velocity maximum and minimum, with the acoustic velocity shown for reference.

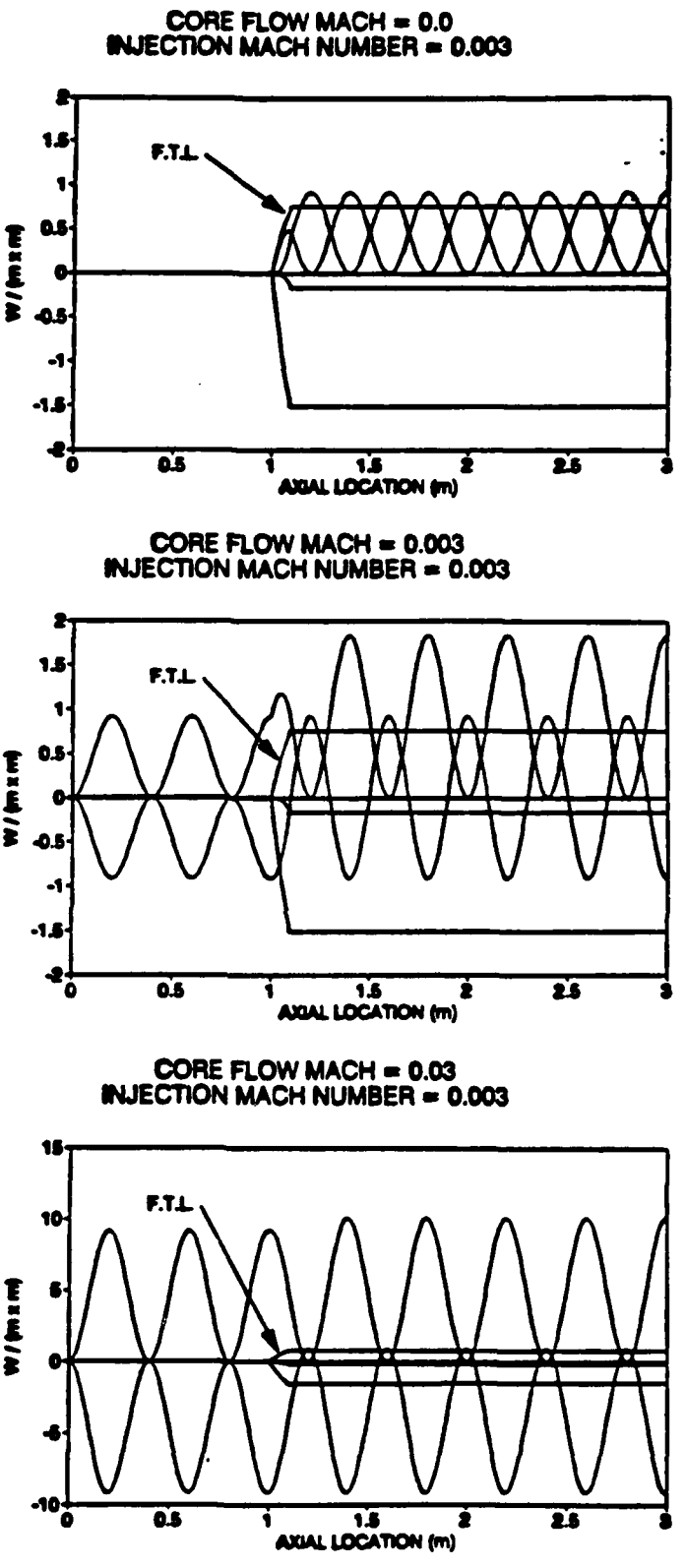

Figure 6. Flow turning loss and remaining terms of the acoustic stability equation for 3 cases with varying core flow Mach numbers.

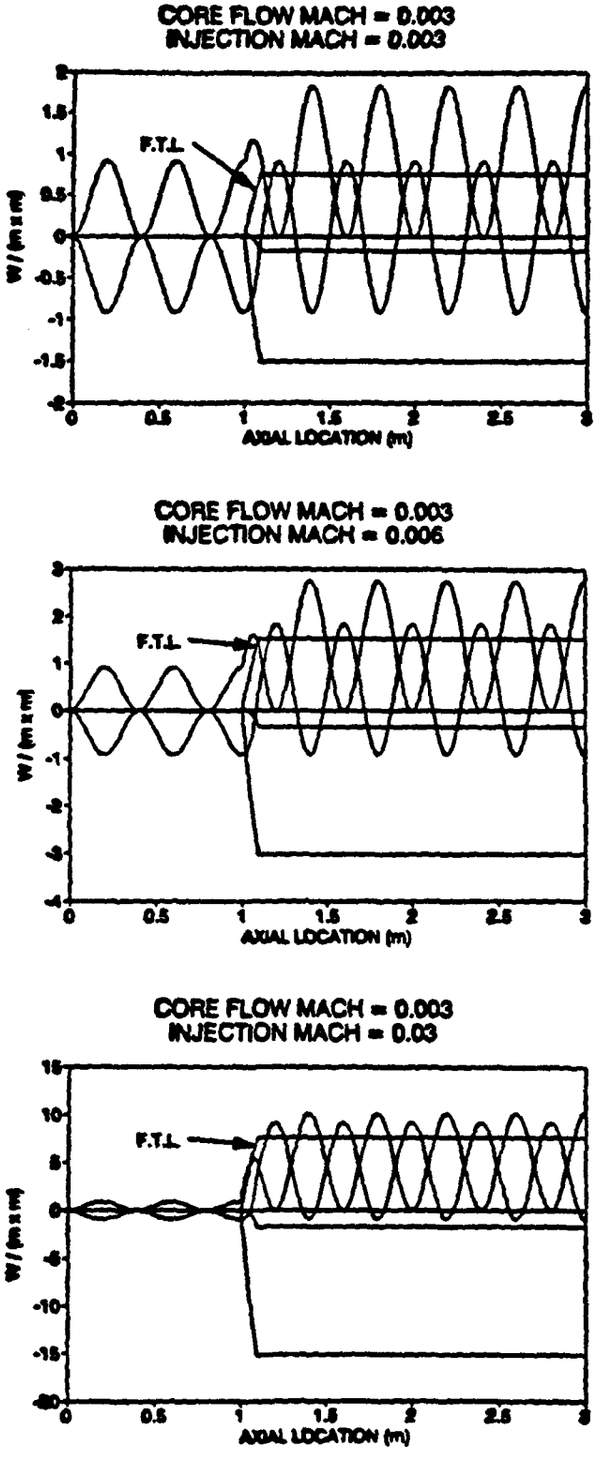

Figure 7. Flow turning loss and remaining terms of the acoustic stability equation for 3 cases with varying side wall injection Mach numbers.

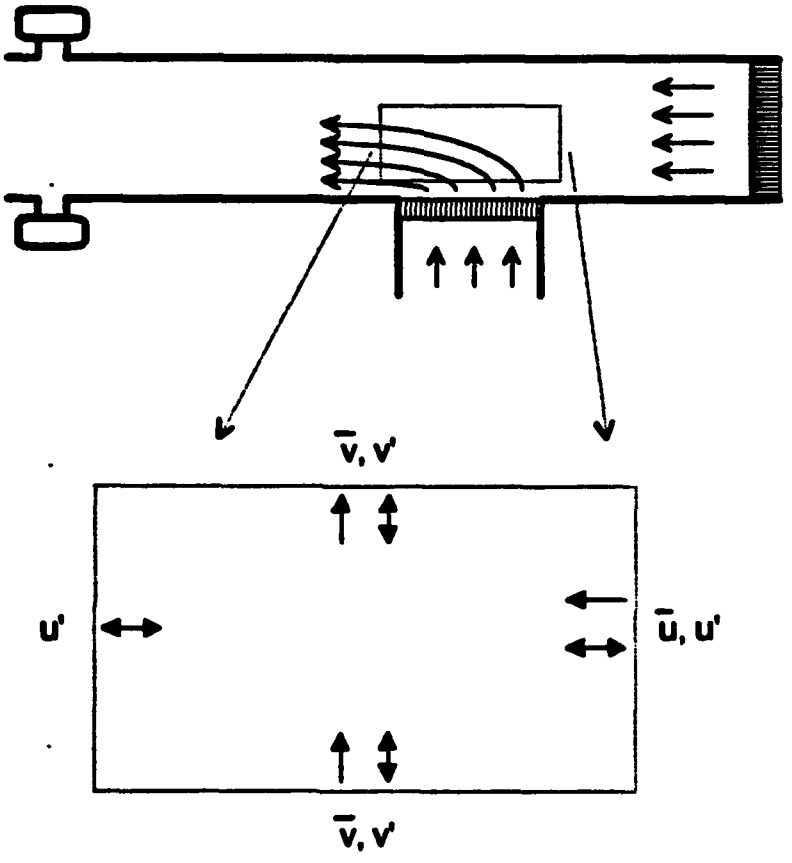

Figure 8. Schematic of the computational configuration used to simulate the experiments showing the measured boundary conditions used.

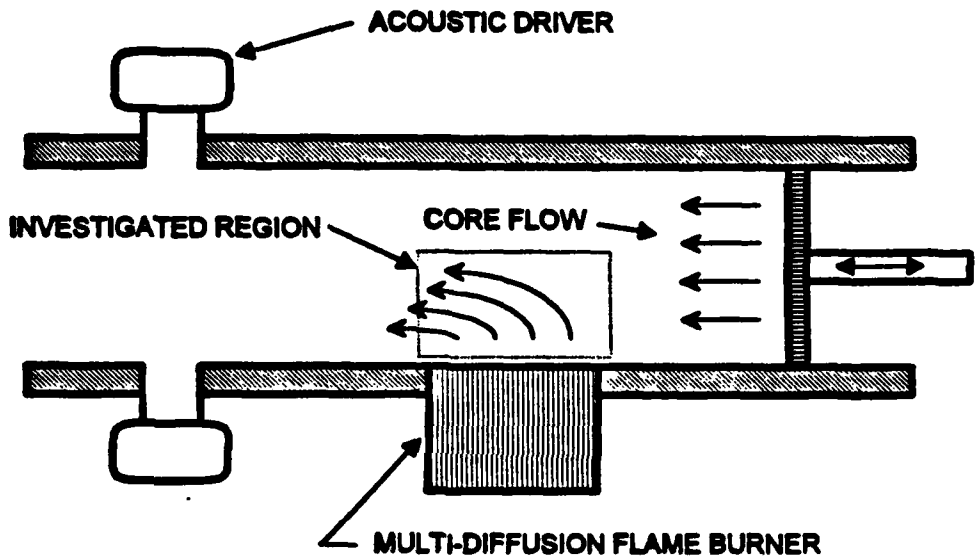

Figure 9. A schematic of the experimental setup utilized in the investigation of flow turning losses.

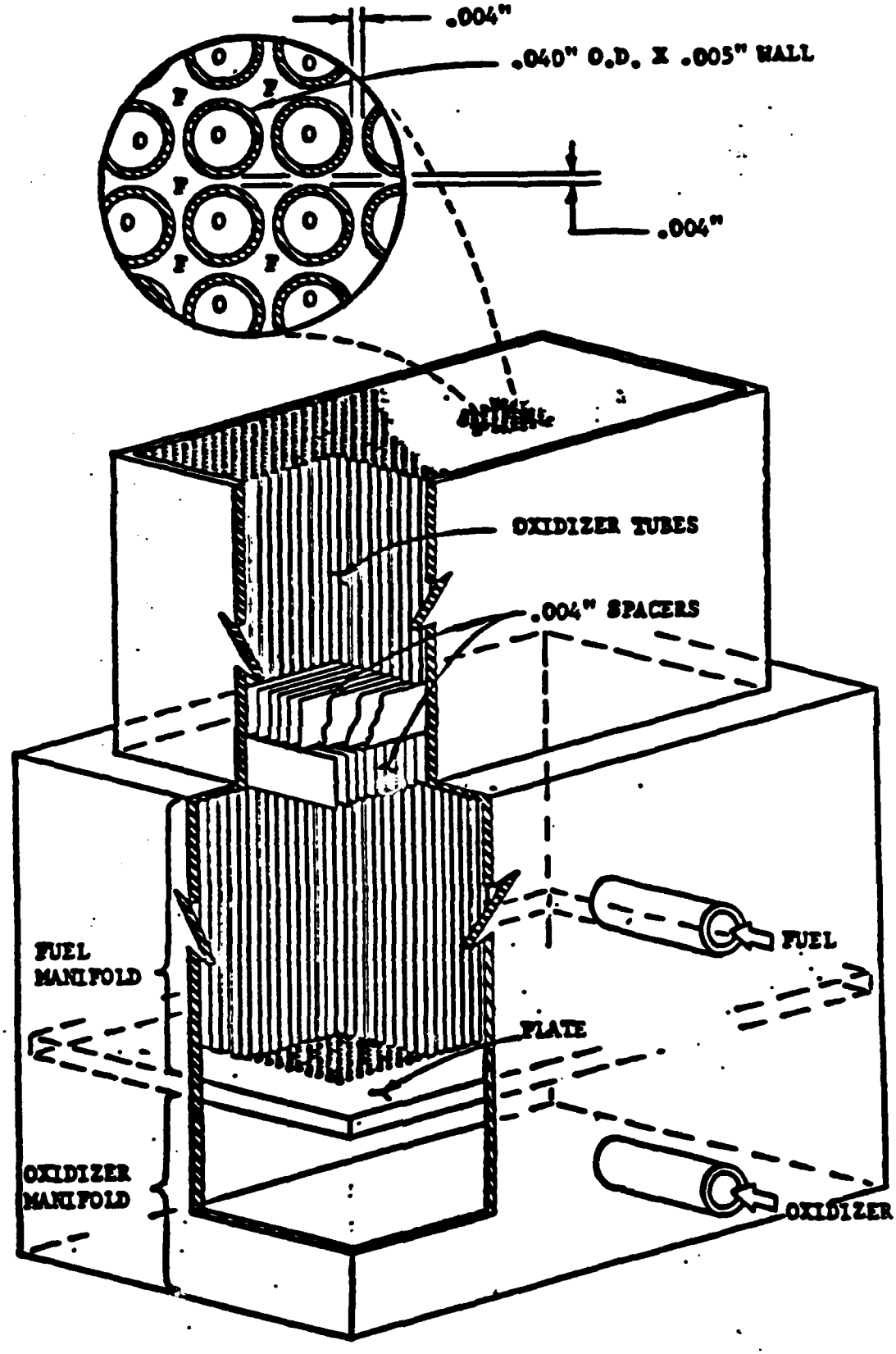

Figure 10. Schematic of the multi-diffusion flame burner.

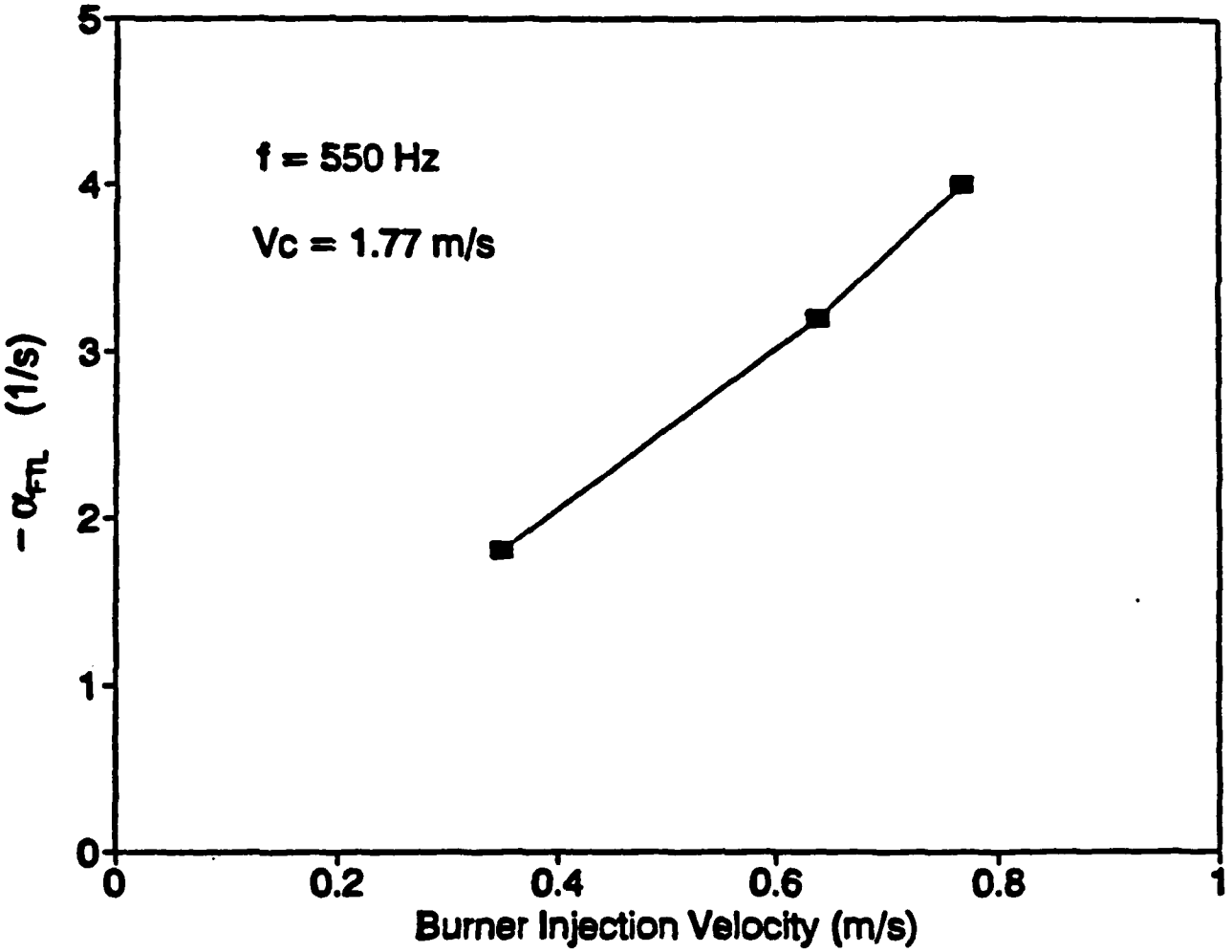

Figure 11. Results of an experiment showing the effect of the side wall injection velocity upon α_{FTL}.

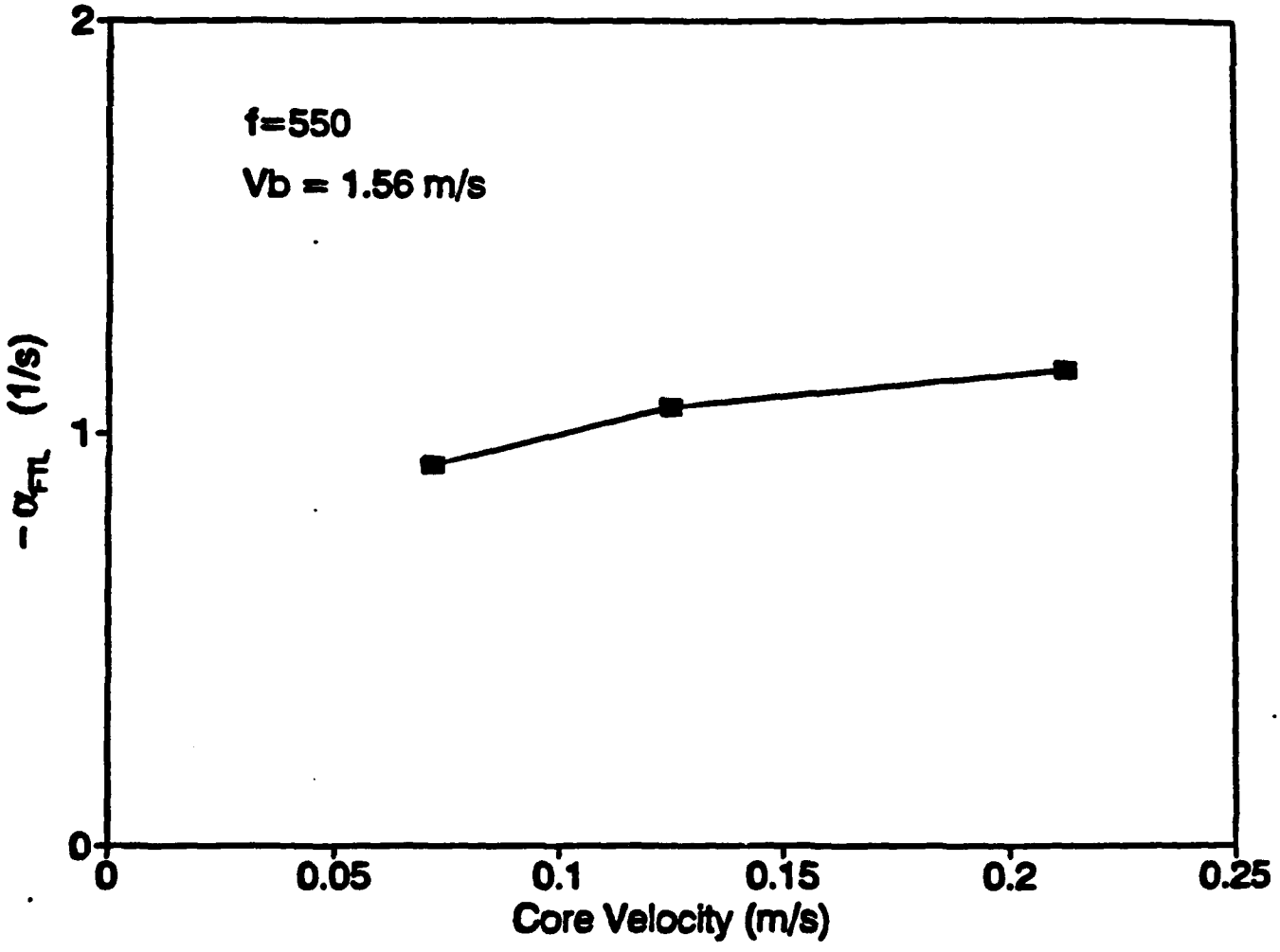

Figure 12. Results of an experiment showing the effect of the mean core flow velocity upon α_{FTL}.

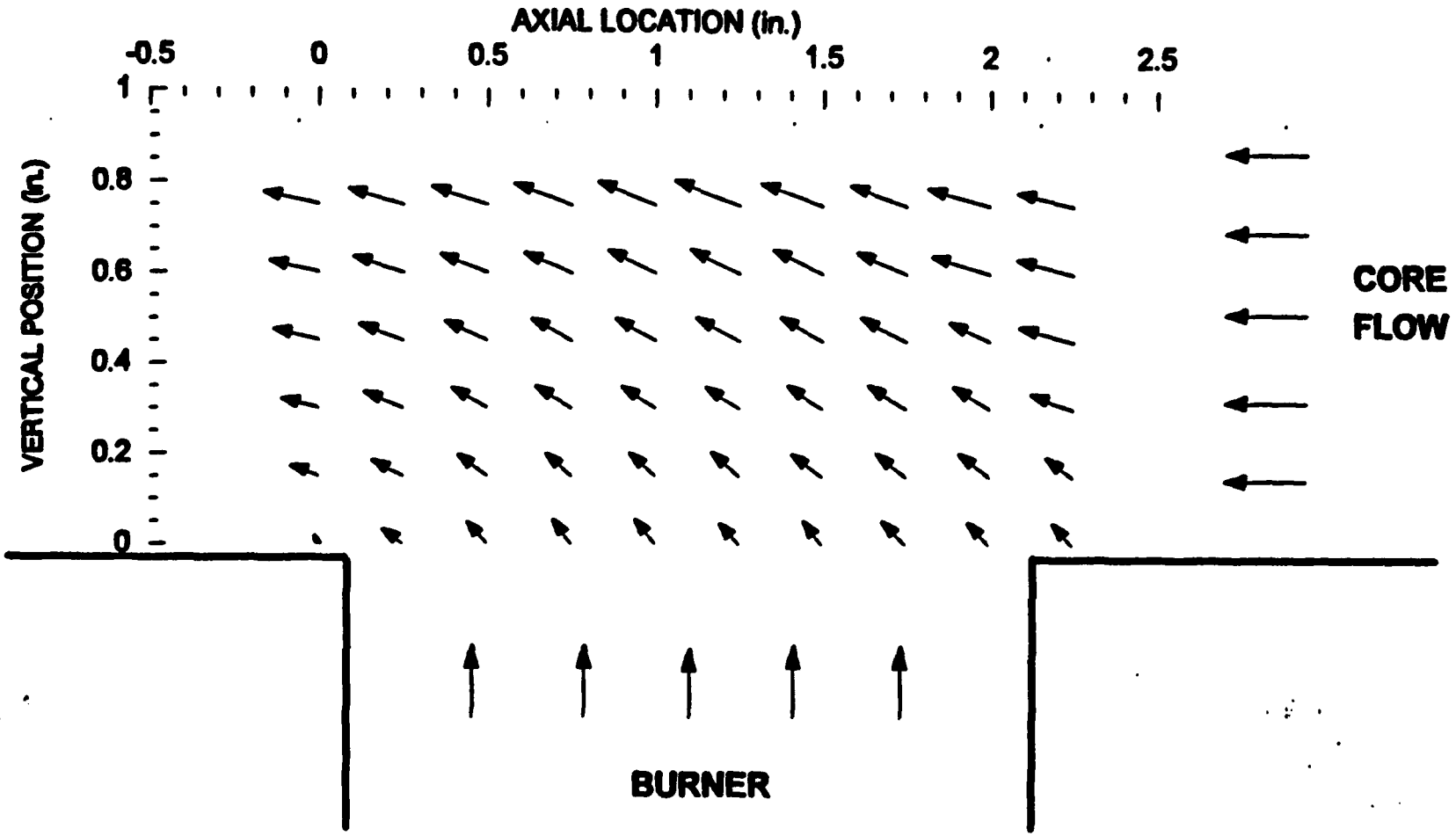

Figure 13. Vector plot of a typical measured mean velocity field in the flow turning region.

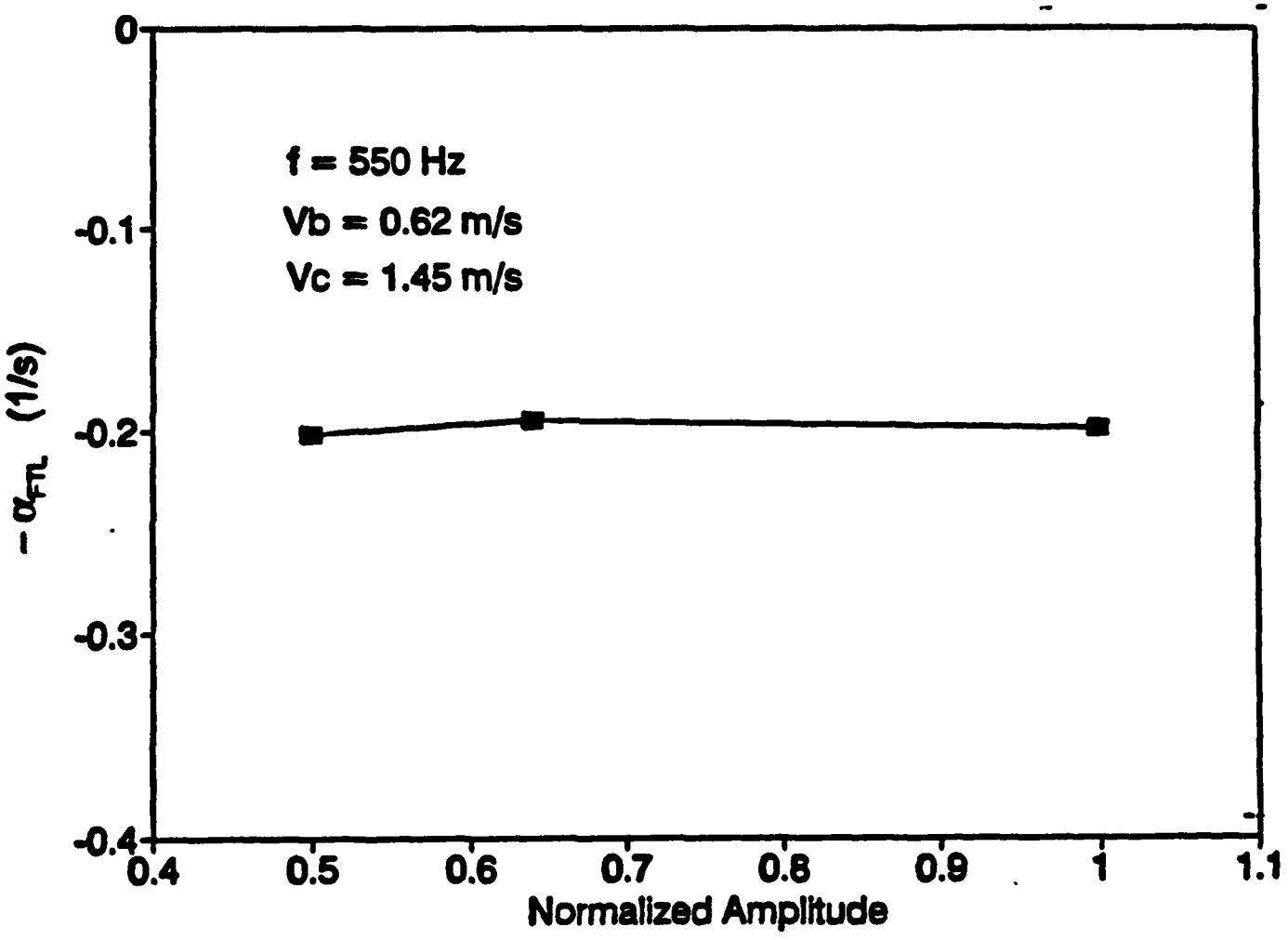

Figure 14. Results of an experiment showing the effect of the amplitude of oscillation upon α_{FTL}.

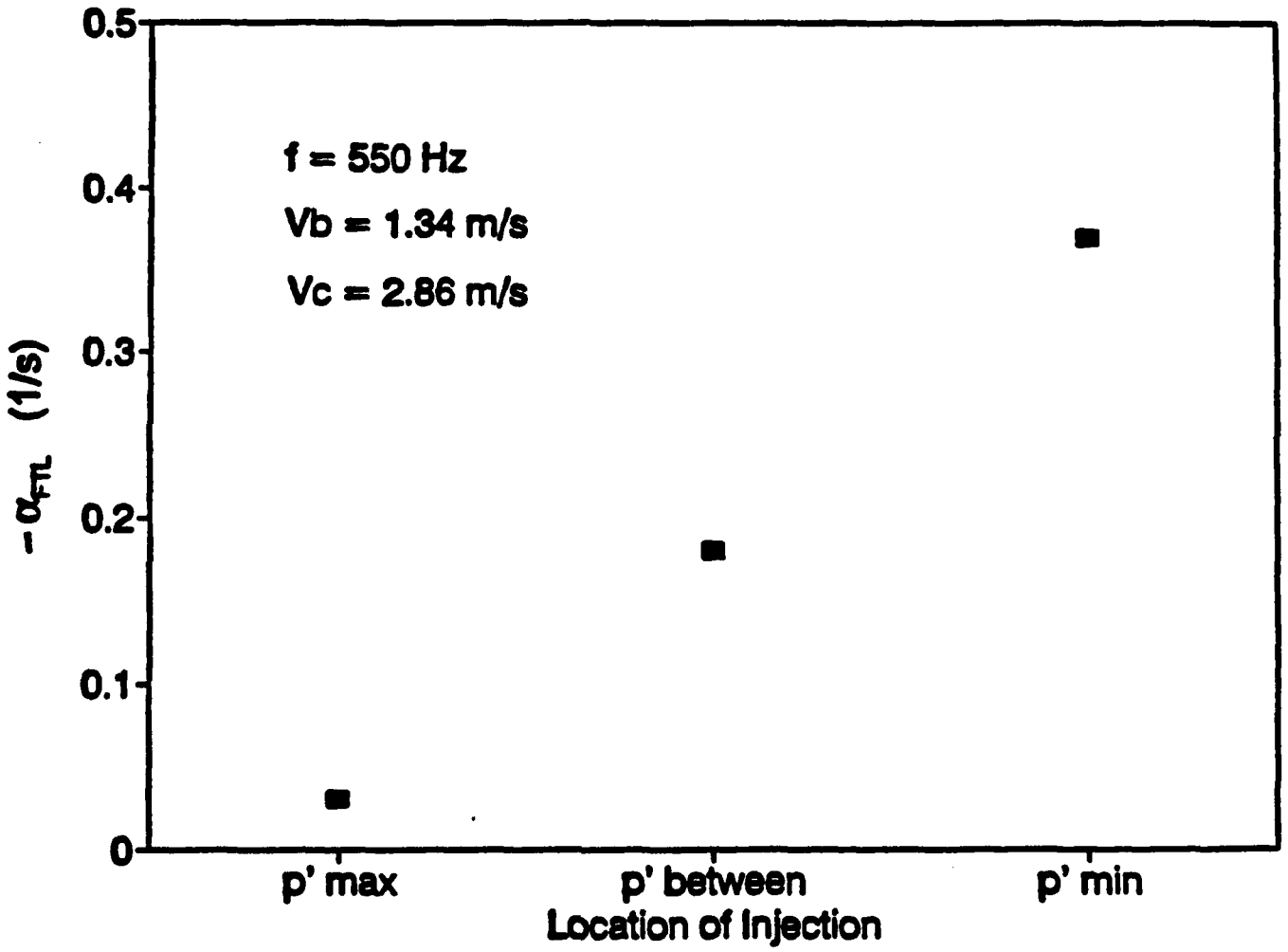

Figure 15. Results of an experiment showing the effect of the location of the flow turning region relative to the standing acoustic wave upon α_{FTL}.

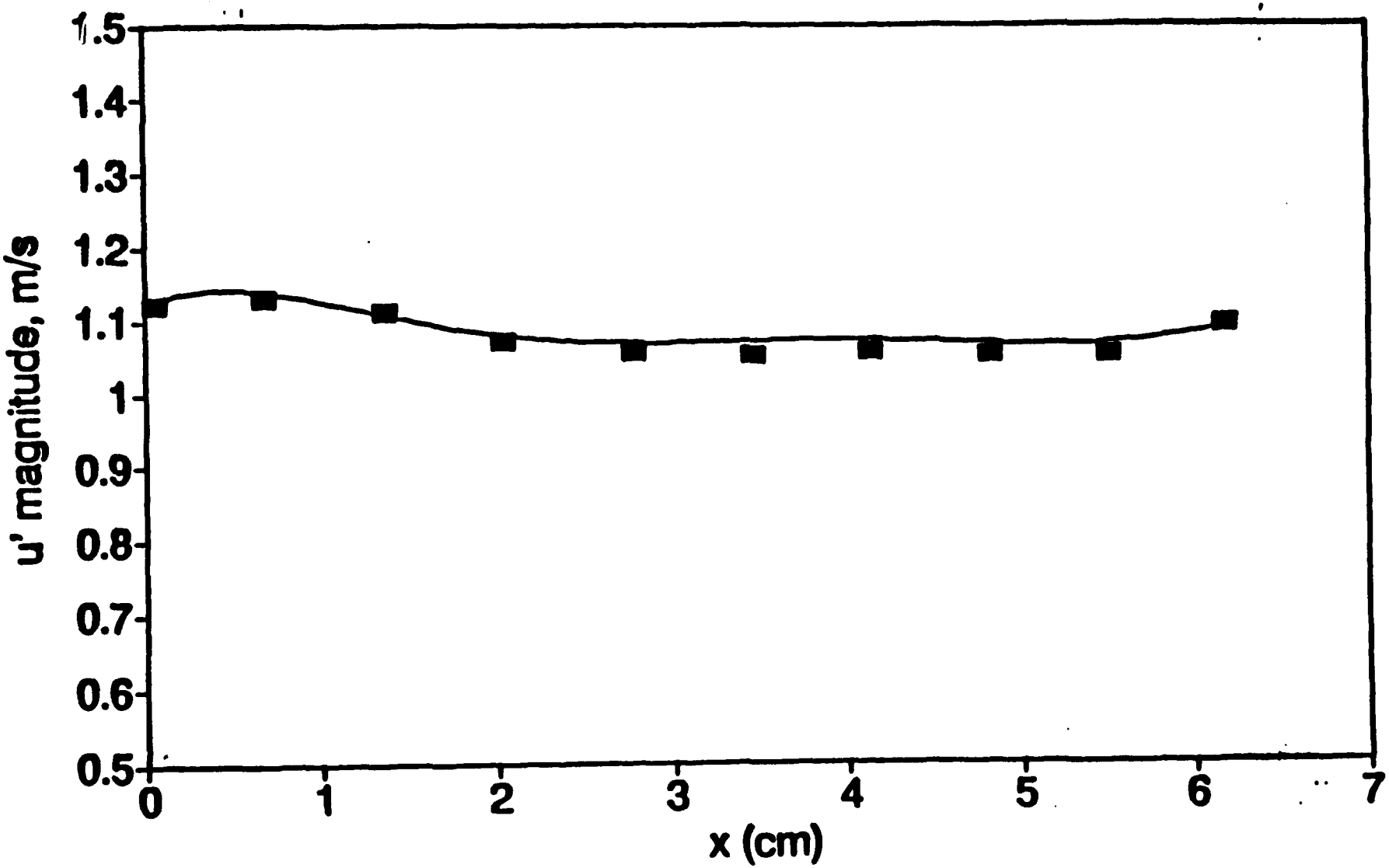

Figure 16. Comparison of the measured and calculated magnitudes of the axial acoustic velocity.

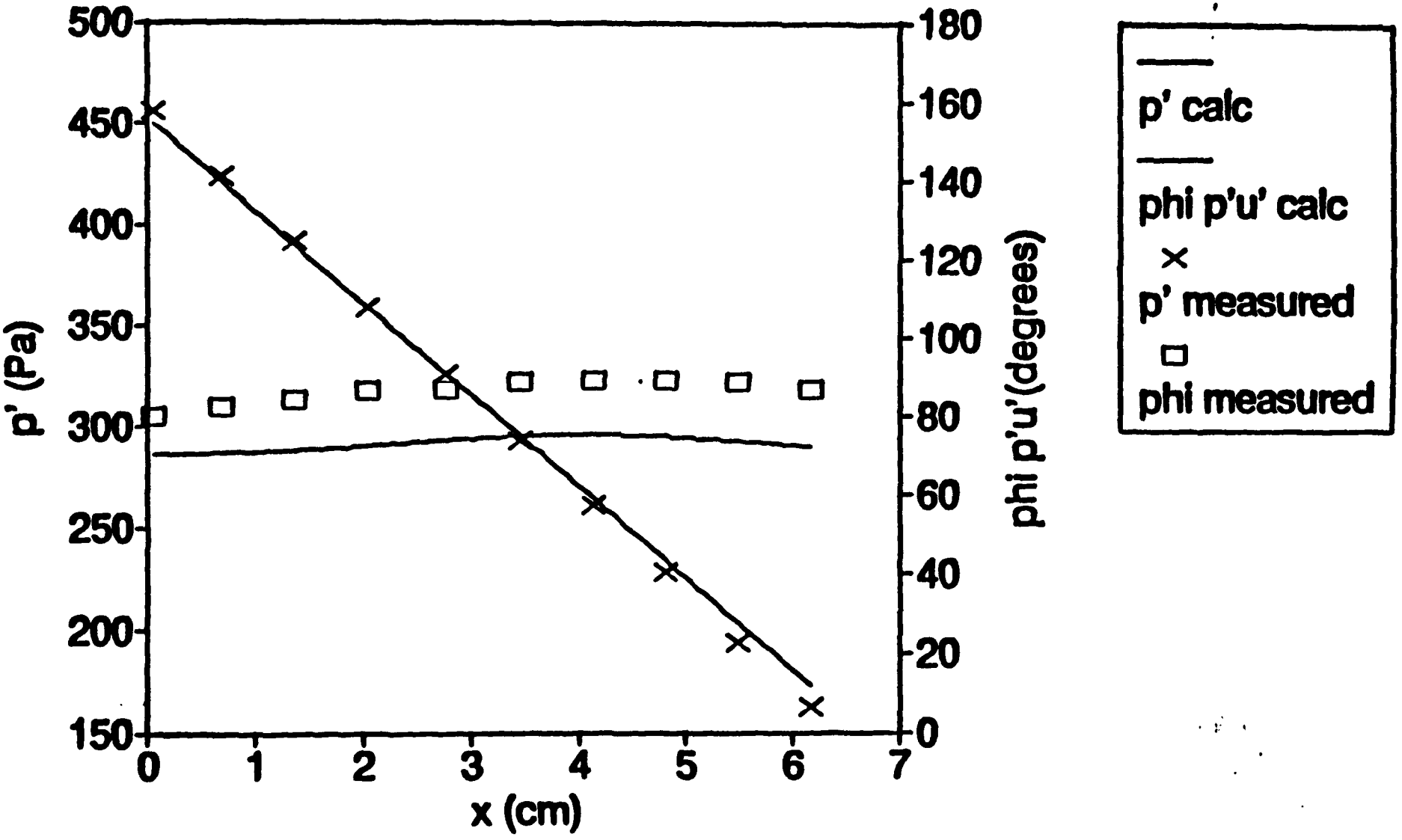

Figure 17. Comparison of the measured and calculated amplitude and phase of the acoustic pressure.

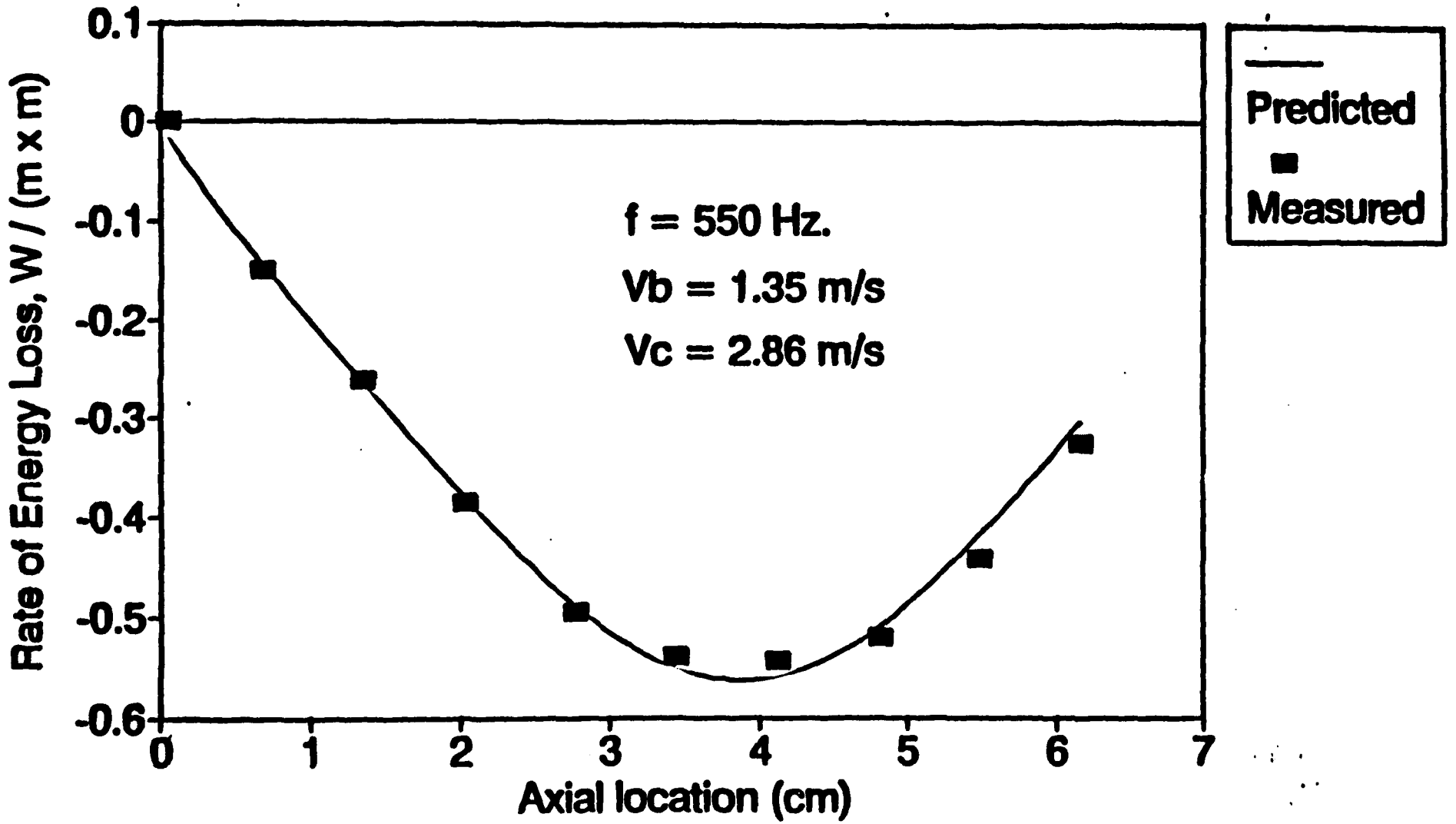

$$\text{Flow Turning Loss} = -\left\langle \frac{1}{H}\int_0^L \left(\langle u_1^2 \rangle, [m_{b0}]_0'' \right) dx \right\rangle_t$$

Figure 18. Comparison of the calculated and measured values of the flow turning loss term.

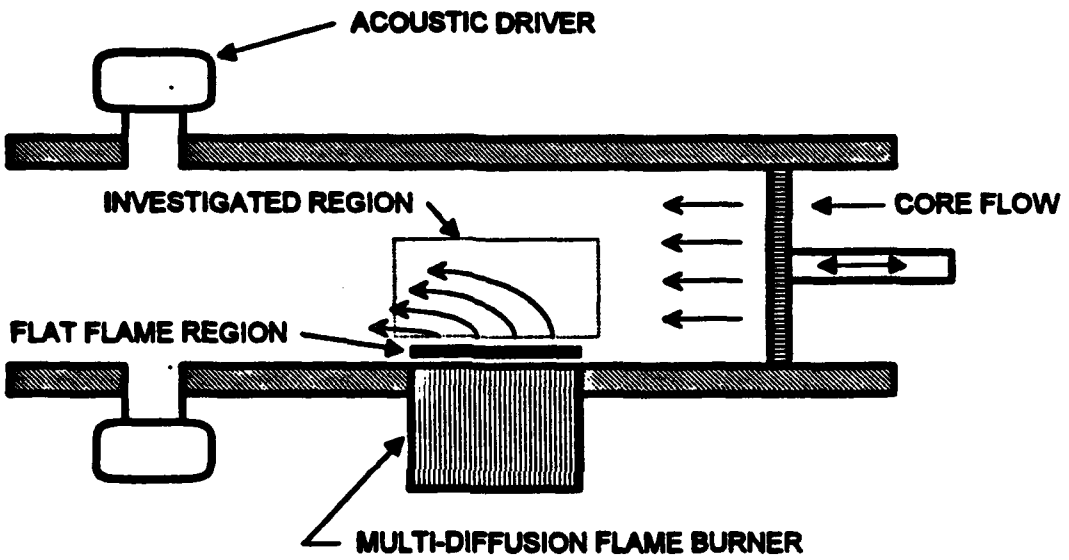

Figure 19. A schematic of the experimental setup and the location of the investigated region.

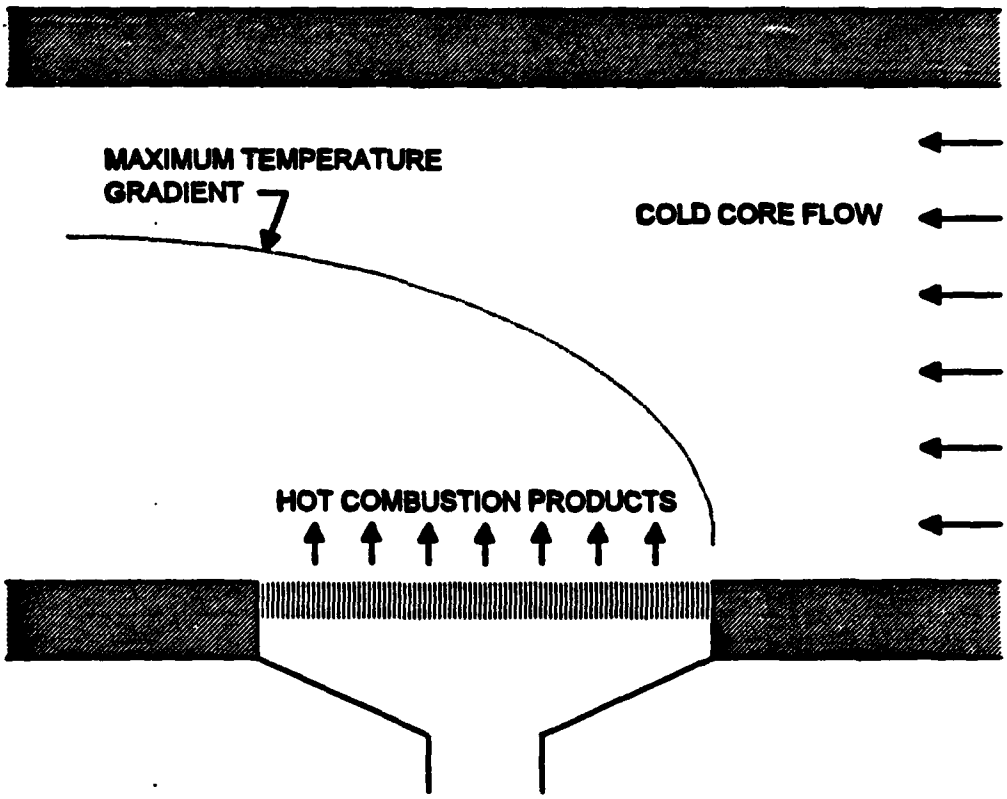

Figure 20. .Description of the mean temperature gradients observed in the experimental setup.

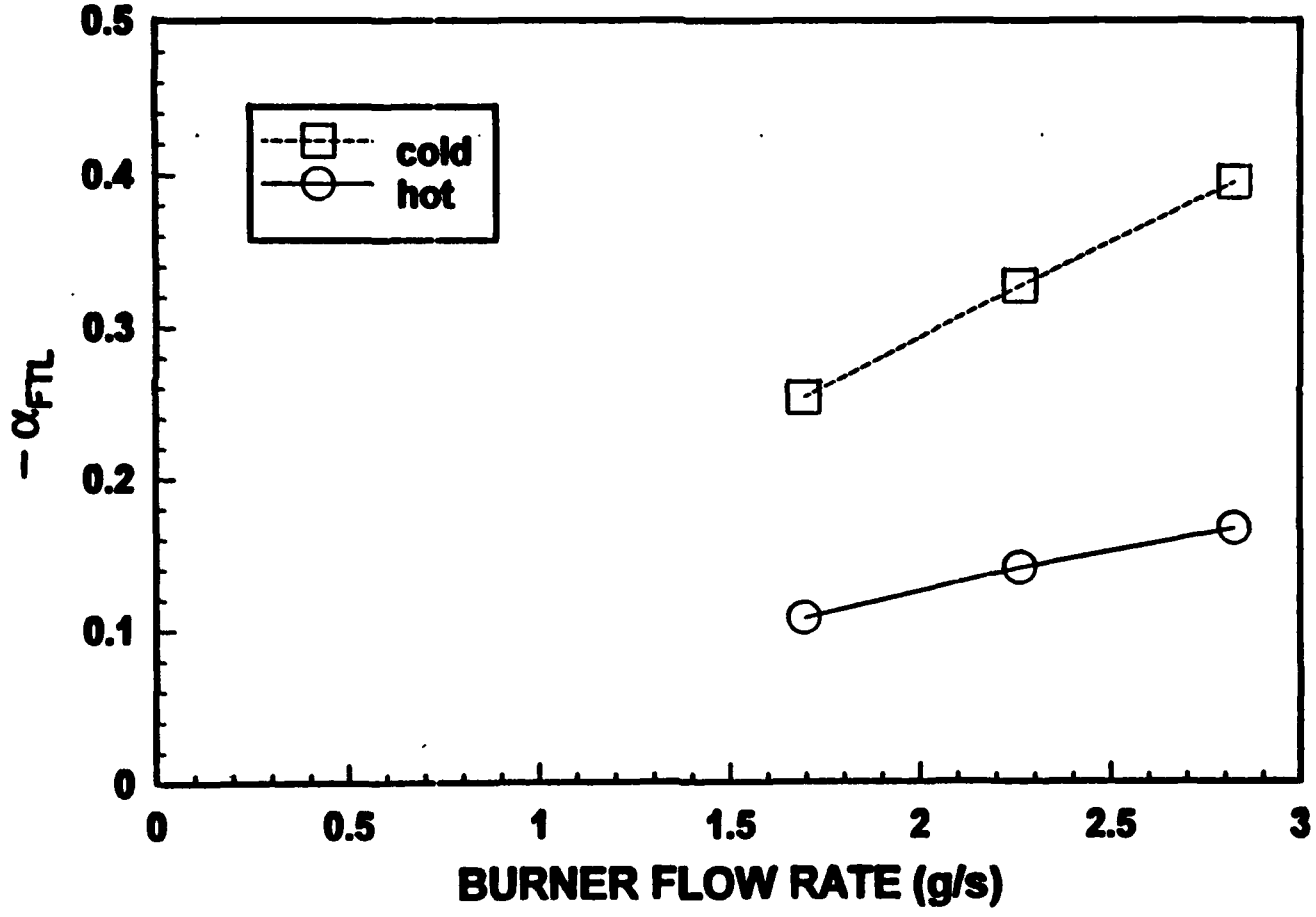

Figure 21. Comparison of α_{FTL} measured in hot and cold flow experiments with different mass flow rates through the burner.

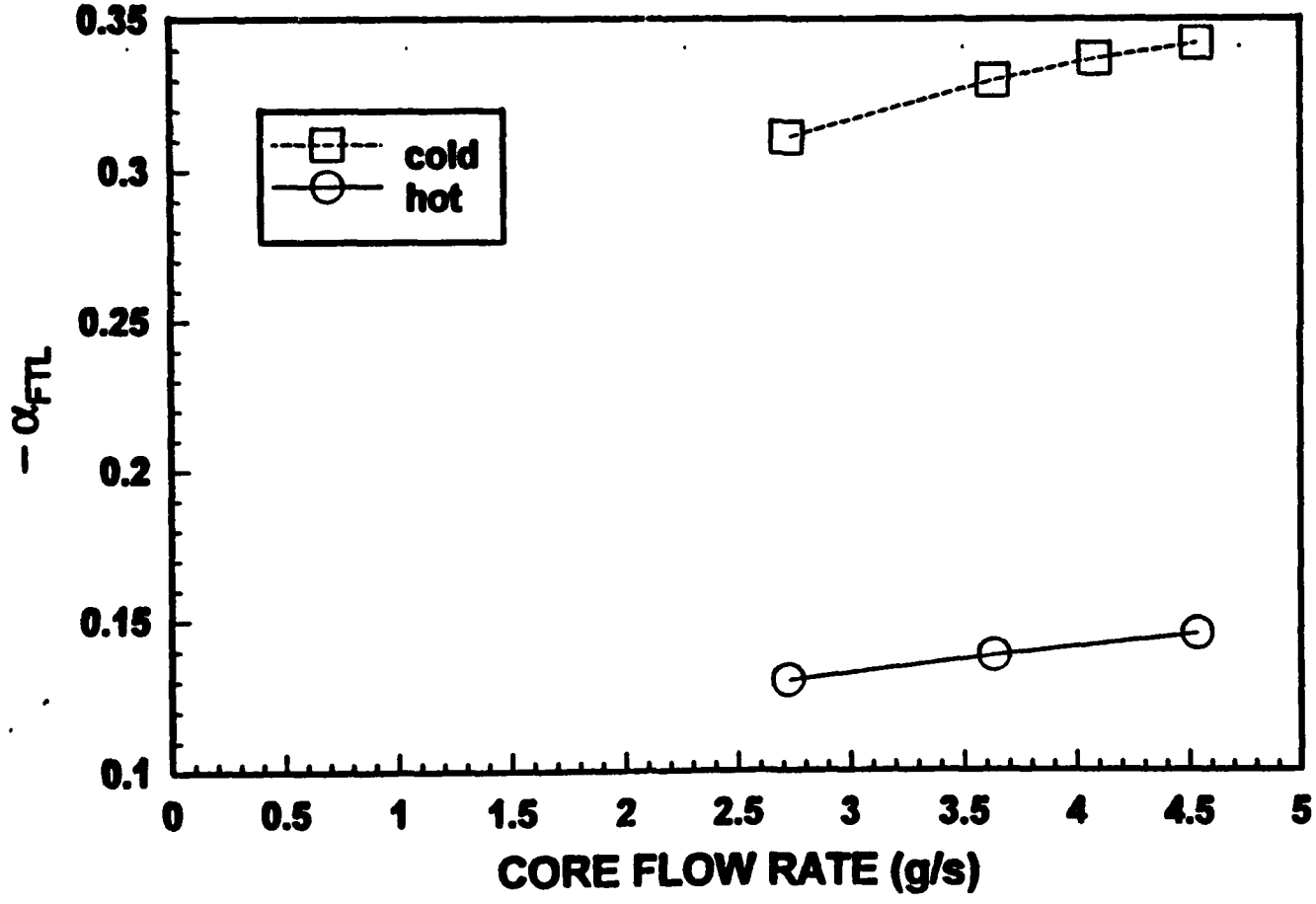

Figure 22. Comparison of α_{FTL} measured in hot and cold flow experiments with different core mass flow rates.

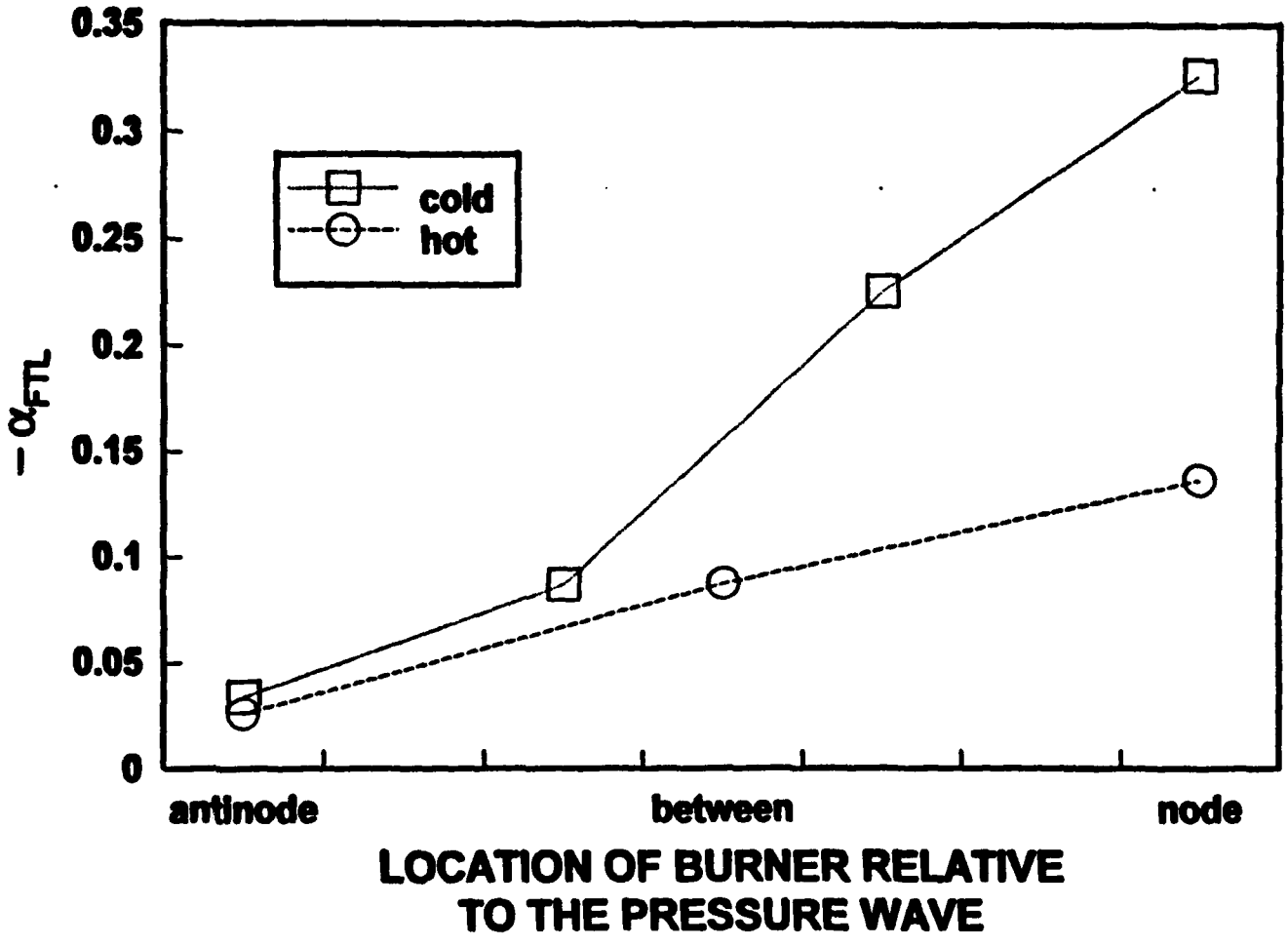

Figure 23. Comparison of α_{FTL} measured in hot and cold flow experiments with the burner at different locations relative to the standing acoustic wave.

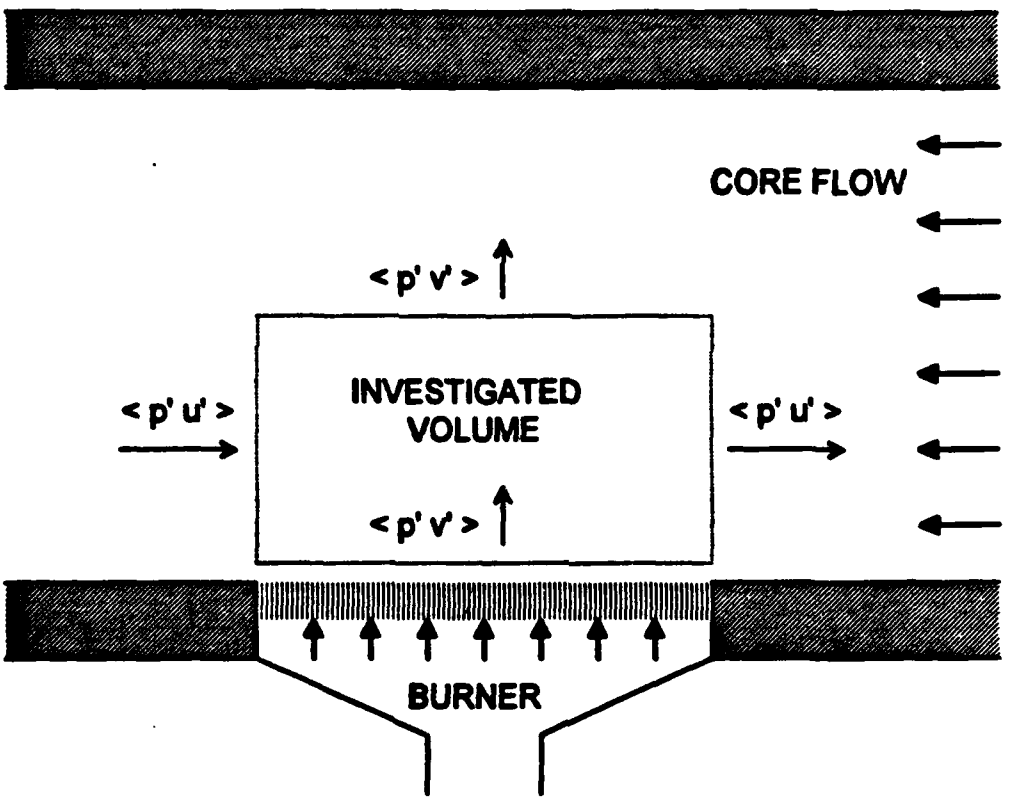

Figure 24. Measurements used for determining the acoustic intensity entering and leaving the investigated region.

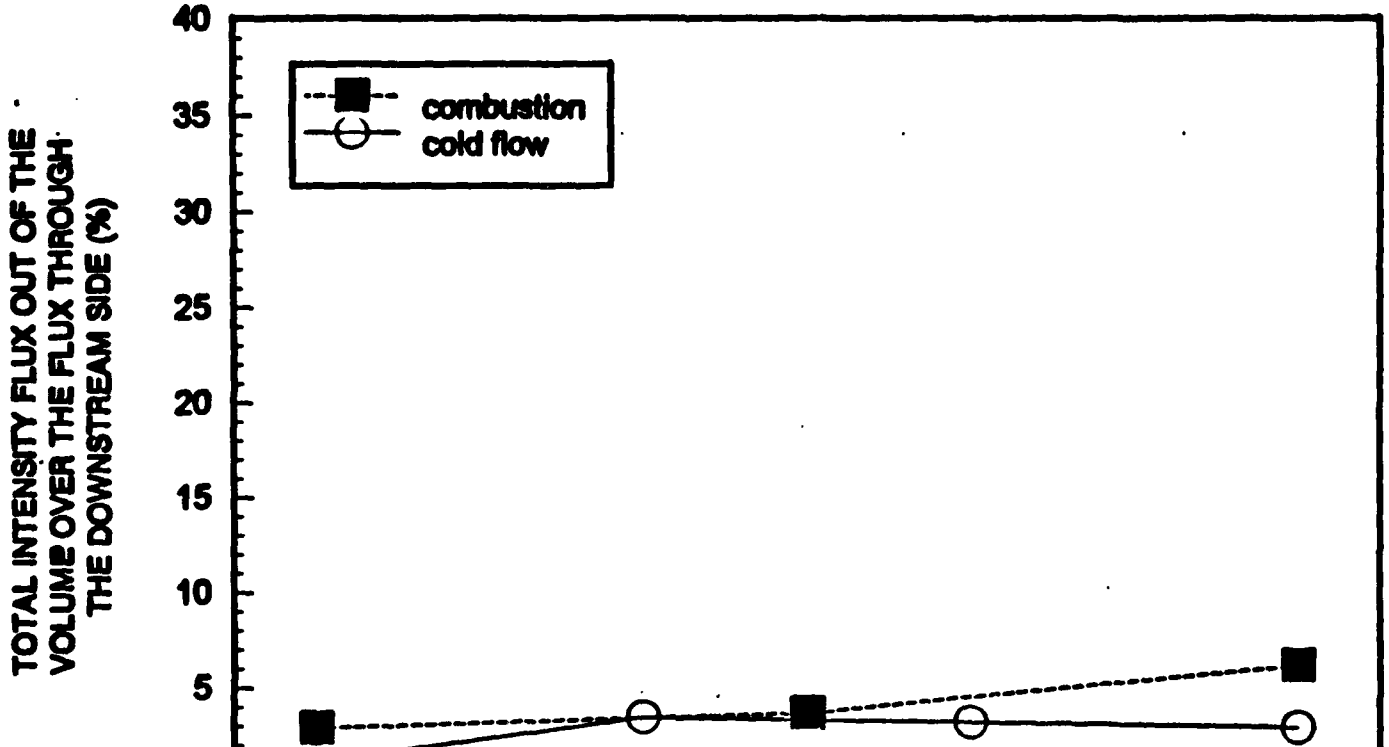

Figure 25. Comparison of the ratio of the total acoustic intensity flux out of the control volume to the flux through the downstream boundary for hot and cold flow cases.

PROFESSIONAL INTERACTIONS

A. Professional Personnel:

Dr. Ben T. Zinn, Regents Professor
Mr. Brady R. Daniel, Senior Research Engineer
Dr. J. I. Jagoda, Associate Professor
Mr. Lawrence M. Matta, Ph.D. Student

B. Publications:

Matta, L. M. and Zinn, B. T., "Theoretical Study of Flow Turning Losses in the Presence of Mean Temperature Gradients", accepted for presentation at the AIAA 32st Aerospace Sciences Meeting, Reno, NV, January, 1994.

Chen, T. Y., Hegde, U. G., Zinn, B. T., and Daniel, B. R., "Flame Radiation and Acoustic Intensity Measurements in Acoustically Excited Diffusion Flames," Journal of Propulsion and Power, Vol. 9, No. 2, pp. 210-216, March-April 1993.

Matta, L. M. and Zinn, B. T., "Investigation Of Flow Turning Loss In A Simulated Unstable Solid Propellant Rocket Motor", AIAA Paper No. 93-0115, AIAA 31st Aerospace Sciences Meeting, Reno, NV, Jan 11-14, 1993.

Zinn, B. T. and Matta, L. M., "Experimental Investigation Of Flow Turning Losses In Unstable Rocket Motors", 29th JANNAF Combustion Subcommittee Meeting, NASA Langley Research Center, Hampton, VA, Oct. 19-23, 1992.

Matta, L. M., Zinn, B. T., and Daniel, B. R., "Theoretical Investigation of Flow Turning Losses in an Experimental Setup Which Simulates Instabilities in Solid Propellant Rocket Motors", AIAA Paper No. 92-0780, AIAA 30th Aerospace Sciences Meeting, Reno, NV, Jan 6-9, 1992.

Zinn, B. T., Matta, L. M., and Daniel, B. R., "Theoretical Investigation of Flow Turning Losses in Unstable Solid Propellant Rocket Motors", 28th JANNAF Combustion Meeting, San Antonio, TX, Oct. 28 - Nov. 1, 1991.

C. Presentations:

"Investigation Of Flow Turning Loss In A Simulated Unstable Solid Propellant Rocket Motor", AIAA Paper No. 93-0115, AIAA 31st Aerospace Sciences Meeting, Reno, NV, Jan 11-14, 1993.

"Experimental Investigation Of Flow Turning Losses In Unstable Rocket Motors", 29th JANNAF Combustion Subcommittee Meeting, NASA Langley Research Center, Hampton, VA, Oct. 19-23, 1992.

"Theoretical Investigation of Flow Turning Losses in an Experimental Setup Which Simulates Instabilities in Solid Propellant Rocket Motors", AIAA Paper No. 92-0780, AIAA 30th Aerospace Sciences Meeting, Reno, NV, Jan 6-9, 1992.

"Theoretical Investigation of Flow Turning Losses in Unstable Solid Propellant Rocket Motors", 28th JANNAF Combustion Meeting, San Antonio, TX, Oct. 28 - Nov. 1, 1991.

APPENDIX

AIAA 92-0780
Theoretical Investigation of Flow Turning Losses in an Experimental Setup Which Simulates Instabilities in Solid Propellant Rocket Motors

L. M. Matta, B. T. Zinn, and B. R. Daniel
Georgia Institute of Technology
Atlanta, GA

30th Aerospace Sciences
Meeting & Exhibit
January 6-9, 1992 / Reno, NV

THEORETICAL INVESTIGATION OF FLOW TURNING LOSSES IN AN EXPERIMENTAL SETUP WHICH SIMULATES INSTABILITIES IN SOLID PROPELLANT ROCKET MOTORS*

L. M. Matta, B. T. Zinn†, and B. R. Daniel
Georgia Institute of Technology
Atlanta, Georgia

Abstract

The acoustic loss mechanism known as "flow turning loss" results from the interaction between the mean flow of the combustion products that enter the combustion chamber and the longitudinal acoustic sound field in an unstable solid rocket motor. Although the flow turning loss is incorporated in state of the art stability codes of solid rocket motors, the existence of this loss has never been adequately verified experimentally. This paper describes a theoretical investigation that has been used to guide the development of an experimental approach for the determination of the flow turning loss. First, the existence of the flow turning loss term in the one-dimensional stability equation was verified using an independent energy balance approach. Next, a theoretical model that could be used to determine the flow turning loss from measured data was developed. An equation describing the acoustic stability of the experimental setup in terms of measurable time averaged and fluctuating quantities was derived from the conservation equations. Finally, the governing equations for the experimental setup were numerically integrated and the solutions substituted into the developed acoustic stability equation to determine the behavior of the various terms that appear in the equation and whether the numerical solution satisfies the developed expression for the growth rate of the oscillations in the experiment. Calculations were carried out for a number of different experimental configurations and operating conditions which showed excellent agreement between the results of the numerical simulation and the developed stability equation.

Introduction

In order to eliminate or reduce the the occurrence of combustion instabilities in solid propellant rocket motors, the processes that add or remove energy from the oscillations must be accurately accounted for in a stability analysis. To attain this goal, an understanding of these processes must be developed. It is generally accepted that the energy required to initiate and maintain the instability is supplied by the combustion process. It is also recognized that nozzle damping, viscous dissipation, heat transfer, and "flow turning" are processes that remove energy from the acoustic field. This study is concerned with the understanding and quantification of the damping provided by the "flow turning" process.

Flow turning losses in an unstable rocket motor are caused by the interaction of the radially directed flow of combustion products that leave the burning propellant surface with the axial acoustic field. The existence of this flow turning loss was first predicted by Culick[1]. Although this flow turning loss is currently incorporated in state of the art stability models that predict the performance of solid propellant rockets, its existence has never been quantitatively verified. Previous efforts[2,3] under this program and elsewhere to measure the flow turning loss have failed because the quantities that needed to be measured were of the same order as the accuracy of the measurement techniques. Consequently, this theoretical study has been undertaken to determine whether the previously developed expression for the flow turning loss is accurate and whether the previous experimental studies failed to account for all the necessary terms in their evaluation of the flow turning loss, therefore giving erroneous results.

In the initial phase of this program[2] an attempt was made to measure the flow turning loss within a set of control volumes where flow turning occurred. This procedure required that an acoustic energy balance be performed on the investigated control volume. In this case, the necessary acoustic energy fluxes were determined from measurements of the classical acoustic energy flux p'^*u', where p' and u' are the acoustic pressure and velocity, respectively, across all the boundaries of the investigated control volume. Since no other sources or sinks of acoustic energy were present within the investigated control volumes, any net loss of acoustic energy was attributed to flow turning. Unfortunately, the losses measured by this procedure were of the same order as the experimental errors and, consequently, could not be trusted. It should be also noted that a related study by Hersch and Tso[3] also failed to provide reliable results due to experimental inaccuracies. The theoretical study reported herein was stimulated by the failure of all studies to date to accurately measure the flow turning loss.

The purpose of this investigation is to determine the causes of Chen's[2] failure to measure the flow turning loss and to propose an alternate experimental approach. First, in order to verify the existence of the flow turning loss, a one-dimensional acoustic stability equation was developed using an energy balance approach similar to that used by Cantrell and Hart[4]. The analysis was based on explicit considerations of the mass, momentum, and acoustic energy fluxes at the control volume boundaries. It involved consideration of the first and second order perturbations of the acoustic quantities. The consideration of second order quantities is necessary for proper evaluation of terms of the order of the acoustic energy. The analysis started with an expansion of the energy equation to second order in the acoustic perturbations. Next, second order expansions of the mass and momentum conservation equations were used to modify the energy equation. This analysis yielded an

* Work performed under AFOSR Grant/Contract No. APOSR-91-0160; Dr. Mitat Birkan Contract Monitor.
† Regent's Professor, Aerospace Engineering, Fellow AIAA

expression for the growth rate α of the unstable wave that is independent of any terms involving second order acoustic quantities. The resulting stability equation is similar to that originally derived by Culick[1] using a different theoretical approach.

Subsequently, in order to develop a theoretical model that could be used to guide the development of an alternate experimental approach for determining the flow turning loss, an analysis was developed that allows for the expansion of all dependent variables (e.g., the pressure) in terms of time averaged and fluctuating quantities similar to those measured in related experiments. For example, the pressure is described by the following expression:

$$p = \bar{p} + p'$$

where $\bar{p}$ is the time average of the measured pressure, p. These dependent variables were substituted into the mass and momentum conservation equations that were then manipulated to derive an acoustic stability equation in terms of the more readily measurable time averaged and fluctuating quantities.

The developed experimental setup that this theoretical investigation aims to describe is shown in Fig. (1). It consists of a 2.5 meter long, 3.75 cm x 7.5 cm duct with the multi-diffusion flame burner (MDFB) shown in Fig. (2) installed on the bottom wall. Though initial experiments will be performed using cold flow, the MDFB can be used to simulate the behavior of a gas phase solid propellant flame. The MDFB consists of 1537 hypodermic tubes arranged in a 29 x 53 matrix. During hot flow experiments, oxidizer flow is supplied through the hypodermic tubes, simulating the flow of combustion products from burning oxidizer particles (e.g., ammonium perchlorate) in a composite solid propellant, and the fuel is supplied through the spaces between the hypodermic tubes, simulating the flow of pyrolysis products from the fuel binder. In cold flow experiments, room temperature air is supplied through both the tubes and the surrounding spaces. Two acoustic drivers attached to opposing duct walls just upstream of the exit plane are used to excite a standing longitudinal acoustic wave in the duct, simulating an axial instability in a rocket motor. Flow is injected at the upstream end of the duct to simulate the axial core flow in a rocket motor. This head end injector is made of a porous plate that behaves as an acoustically 'hard' termination. The location of the MDFB relative to the acoustic field can be changed by axial translation of the porous plate. Directly above the MDFB, the the flow through the burner turns in the direction of the core flow (i.e., along the axis of the duct). This is where flow turning losses are expected to be observed. Optical windows in this region allow LDV measurements of acoustic and mean velocities and a water cooled pressure probe allows acoustic pressure measurement.

To determine the behavior and relative orders of magnitude of the various terms that appear in the developed stability expression, a simple numerical simulation of the experimental setup that will be used to study the flow turning loss was carried out. The simulation required the derivation and numerical solution of the perturbed mass and axial momentum conservation equations for the proposed experimental setup. The derived solutions were substituted into the developed acoustic stability equation to determine the relative orders of magnitude of the various terms that appear in the equation and whether the numerical solution satisfies the developed expression for the growth rate α of the oscillations in the "forced" experiment. These calculations were carried out for a number of different experimental configurations and operating conditions, and in all cases excellent agreement between the results of the numerical simulation and the developed stability equation was obtained.

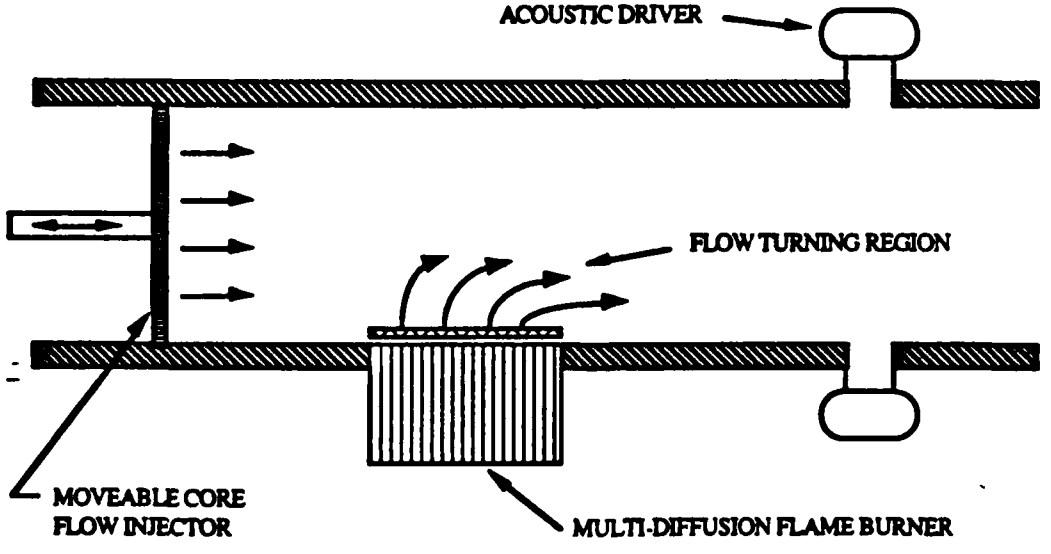

Figure *. A schematic of the experimental setup used in the flow turning investigation.

Theoretical Formulation

Energy Balance

The initial goal of this investigation was to analytically verify the existence of the flow turning loss by deriving an equation for the acoustic stability of a combustor by an approach different than that used by Culick. In order to make the investigation as straight forward as possible, and make it applicable to the proposed experimental setup (see Fig. 1), the investigated geometry consisted of a 2-D rectangular duct of height H and length L. The formulation is based upon a procedure developed by Cantrell and Hart[4]. It begins with considerations of the mass, momentum, and energy conservation equations. The utilized two dimensional mass and momentum conservation equations are:

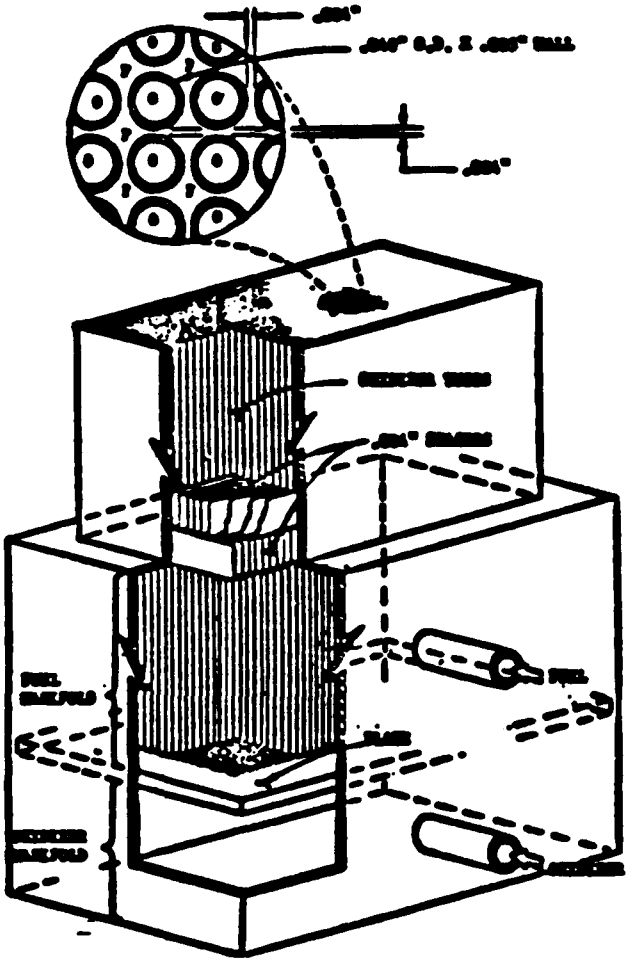

Figure 2. Schematic of the multi-diffusion flame burner used to simulate combustion of composite solid propellant fuels during flow turning experiments.

Mass:

$$\frac{\partial \rho}{\partial t} + \nabla \cdot \mathbf{m} = 0 \tag{1}$$

Momentum:

$$\frac{\partial \vec{V}}{\partial t} + \nabla\left(\frac{\vec{V}\cdot\vec{V}}{2}\right) + \frac{1}{\rho}\nabla p = \left(u\frac{\partial u}{\partial y}\right)\hat{j} + \left(v\frac{\partial v}{\partial x}\right)\hat{i} - \left(u\frac{\partial v}{\partial x}\right)\hat{j} - \left(v\frac{\partial u}{\partial y}\right)\hat{i} \tag{2}$$

where ρ is the density, u and v are the axial and vertical components of the velocity vector V, p is the pressure and m is the mass flux vector ρV. This particular form of the momentum equation has been chosen for its convenience later in the analysis. Assuming that the flow is isentropic, Eq. (2) becomes

$$\frac{\partial \vec{V}}{\partial t} + \nabla h_T = \left(u\frac{\partial u}{\partial y}\right)\hat{j} + \left(v\frac{\partial v}{\partial x}\right)\hat{i} - \left(u\frac{\partial v}{\partial x}\right)\hat{j} - \left(v\frac{\partial u}{\partial y}\right)\hat{i} \tag{3}$$

where h_T is the total enthalpy per unit mass. As a result of the isentropic flow assumption, this analysis cannot account for losses due to particle damping and heat transfer, or gas phase heat addition by combustion processes. In a more general treatment, an attempt must be made to consider non-isentropic effects due, for example, to heat transfer and viscous processes.

The development of the acoustic stability equation by an energy balance approach starts with the following form of the energy equation

$$\frac{\partial}{\partial t}(\rho h_T - p) = -\nabla \cdot (\mathbf{m} h_T) \tag{4}$$

Since the acoustic energy is a second order acoustic quantity, all first and second order terms must be retained in the analysis while third order and higher order terms may be neglected. Thus, Eq. 4 is expanded to second order and time averaged to yield

$$\left\langle \frac{\partial}{\partial t}(\rho h_T - p)_2 \right\rangle_t = -\left\langle \nabla \cdot (m_2 h_{T0}) + \nabla \cdot (m_1 h_{T1}) + \nabla \cdot (m_0 h_{T2}) \right\rangle_t \tag{5}$$

where the quantities inside a bracket $\langle\rangle$ are averaged over the subscripted variable and the numerical subscripts indicate the order of term. To eliminate the dependence upon y, Eq. (5) is averaged over the height (i.e., the y direction) of the constant area duct to obtain

$$\left\langle \frac{\partial}{\partial t}(\rho h_T - p)_2 \right\rangle_{t,y} = -\frac{\partial}{\partial x}\left\langle \left((\rho u)_1 h_{T1}\right) \right\rangle_{t,y}$$

$$-\frac{\partial}{\partial x}\left(\left((\rho u)_2 h_{T0}\right)+\left((\rho u)_0 h_{T2}\right)\right)_{t,y}$$

$$+\frac{1}{H}\left\langle\left[\left((\rho v)_2 h_{T0}\right)+\left((\rho v)_1 h_{T1}\right)+\left((\rho v)_0 h_{T2}\right)\right]_0^H\right\rangle_t \qquad (6)$$

where H is the height of the duct.

Equation (6) includes second order terms whose solution are generally not known and difficult to obtain. It is possible, however, to use Eqs. (1) and (3) to eliminate these terms in Eq. (6). In order to accomplish this, some manipulations of Eqs. (1) and (3) must be performed. With this in mind, the zeroth order part of Eq. (3) (i.e., the steady state energy equation) is obtained by retaining all terms that are independent of time and neglecting terms of second order and higher in the mean Mach number, resulting in the following equation:

$$\nabla h_{T0} = 0 \qquad (7)$$

Next, the continuity equation, Eq. (1), was multiplied by Δh_{T0} and the resulting equation added to the product of Eq. (7) and m. The resulting equation was then averaged over y and t to obtain the following equation where all terms of the order of Mach number square or higher were neglected:

$$\frac{\partial}{\partial x}\left(\left((\rho u)_2 h_{T0}\right)\right)_{t,y}+\frac{1}{H}\left\langle\left[\left((\rho v)_2 h_{T0}\right)\right]_0^H\right\rangle_t$$

$$=-\left\langle h_{T0}\frac{\partial \rho}{\partial t}\right\rangle_{t,y} \qquad (8)$$

Another needed equation is obtained by forming the dot product of the second order momentum equation, Eq. (3), with the zeroth order mass flux to obtain the following expression where all terms of the order of Mach number square or higher were neglected:

$$\left\langle\nabla\cdot m_0 h_{T2}\right\rangle_t+\left\langle\frac{\partial}{\partial t}\left(m_0\cdot\vec{V}_2\right)\right\rangle_t=$$

$$\left\langle\left(\rho_0 v_0 u_1\frac{\partial u_1}{\partial y}\right)\hat{j}+\left(\rho_0 u_0 v_1\frac{\partial v_1}{\partial x}\right)\hat{i}\right\rangle_t-$$

$$\left\langle\left(\rho_0 v_0 u_1\frac{\partial v_1}{\partial x}\right)\hat{j}+\left(\rho_0 u_0 v_1\frac{\partial u_1}{\partial y}\right)\hat{i}\right\rangle_t \qquad (9)$$

Equation (9) is now averaged across the duct to yield

$$\frac{\partial}{\partial x}\left(\left((\rho u)_0 h_{T2}\right)\right)_{t,y}+\frac{1}{H}\left\langle\left[\left((\rho v)_0 h_{T2}\right)\right]_0^H\right\rangle_t+$$

$$\left\langle\frac{\partial}{\partial t}\left(\rho_0 u_0 u_2+\rho_0 v_0 v_2\right)\right\rangle_t=$$

$$\left\langle\left(\rho_0 v_0 u_1\frac{\partial u_1}{\partial y}\right)\hat{j}+\left(\rho_0 u_0 v_1\frac{\partial v_1}{\partial x}\right)\hat{i}\right\rangle_{t,y}-$$

$$\left\langle\left(\rho_0 v_0 u_1\frac{\partial v_1}{\partial y}\right)\hat{j}+\left(\rho_0 u_0 v_1\frac{\partial u_1}{\partial y}\right)\hat{i}\right\rangle_{t,y} \qquad (10)$$

Equations (8) and (10), while not physically meaningful in themselves, are in forms that are useful for simplifying the energy equation, Eq. (6). Substitution Eqs. (8) and (10) into Eq. (6), rearranging and simplifying the resulting expression, and integration of the result over the length of the duct, the following equation is obtained:

$$\left\langle\frac{\partial}{\partial t}\int_0^L\left(\frac{p_1^2}{2\rho_0 a_0^2}+\frac{\rho_0 u_1^2}{2}+\frac{p_1 u_0 u_1}{a_0^2}\right)dx\right\rangle_t$$

$$=-\left\langle\left[p_1 u_1+\frac{p_1^2 u_0}{\rho_0 a_0^2}+\rho_0 u_0 u_1^2\right]_0^L\right\rangle_{t,y}$$

$$-\left\langle\frac{1}{H}\int_0^L\left(\left(p_1\right)_y\left[v_1\right]_0^H+\left\langle\frac{p_1}{\rho_0 a_0^2}\right\rangle_y\left[v_0 p_1\right]_0^H\right)dx\right\rangle_t$$

$$-\left\langle\frac{1}{H}\int_0^L\left(\left(\rho_0 u_1\right)_y\left[v_1 u_0\right]_0^H\right)dx\right\rangle_t$$

$$+\left\langle\frac{1}{H}\int_0^L\left(\left(\rho_0 u_1\right)_y\left[v_0 u_1\right]_0^H\right)dx\right\rangle_t$$

$$+\left\langle\frac{1}{H}\int_0^L\left(\left\langle\rho_0 u_1^2\right\rangle_y\left[v_0\right]_0^H\right)dx\right\rangle_t \qquad (11)$$

where L and H are the length and height of the duct and a_0 is the zeroth order speed of sound. Equation (11) is the integral form of a conservation equation for the quantity in the time derivative. It must be made clear that this quantity, which has units of energy, does not represent the total acoustic energy of the system. The lack of a simple physical interpretation of this quantity is the necessary result of the cancellation that resulted from the above described simplifications of Eq. (6).

Letting, for convenience, the energy integral in the above integral equal E^2; that is,

$$E^2=\left\langle\int_0^L\left(\frac{p_1^2}{2\rho_0 a_0^2}+\frac{\rho_0 u_1^2}{2}+\frac{p_1 u_0 u_1}{a_0^2}\right)dx\right\rangle_t \qquad (12)$$

and noting that the growth rate of each of the acoustic energy terms is the same as the growth rate of E^2, then the exponential growth rate α can be obtained from the

following expression:

$$2\alpha = \frac{\left\langle \frac{d\psi}{dt} \right\rangle_t}{(\psi - \psi_0)_t} \tag{13}$$

where ψ is a second order acoustic quantity. Using Eqs. (12) and (13), the following acoustic stability equation is obtained from Eq. (11):

$$2\alpha E^2 = -\left\langle \left[p_1 u_1 + \frac{p_1^2 u_0}{\rho_0 a_0^2} + \rho_0 u_0 u_1^2 \right]_0^L \right\rangle_{t,y}$$

$$-\left\langle \frac{1}{H}\int_0^L \left((p_1)_y \left[\frac{m_{b1}}{\rho_0} \right]_0^H + (u_1)_y [\, m_{b1} u_0]_0^H \right) dx \right\rangle_t$$

$$-\left\langle \frac{1}{H}\int_0^L \left((u_1)_y [\, m_{b0} u_1]_0^H \right) dx \right\rangle_t$$

$$+\left\langle \frac{1}{H}\int_0^L \left((u_1^2)_y [\, m_{b0}]_0^H \right) dx \right\rangle_t \tag{14}$$

where m_b is the mass flux (ρv) out of the walls (where all burning is assumed to take place), which is by definition positive in the positive y direction. This equation is by intent (and not by any obvious choice of groupings) of a form that allows comparison with the acoustic stability equation developed by Culick[1]. Culick's equation, simplified by removing the terms that contain the effects of particulate matter, gas phase combustion, and cross-duct temperature gradients, is

$$2\alpha E_1^2 = -\left\langle \left[\hat{p}_1 \hat{u} + \frac{\hat{p}_1^2 u_0}{\rho_0 a_0^2} \right]_0^L \right\rangle_y$$

$$-\frac{1}{H}\int_0^L \left(\langle \hat{p}_1 \rangle_y \left[\frac{\hat{m}_b}{\rho_0} \right]_0^H + \langle \hat{u}_1 \rangle_y [\, \hat{m}_b u_0]_0^H \right) dx$$

$$-\frac{1}{H}\int_0^L \left(\langle \hat{u}_1 \rangle_y [\, m_{b0} \hat{u}]_0^H - \langle \hat{u}_1^2 \rangle_y [\, m_{b0}]_0^H \right) dx \tag{15}$$

where $\hat{}$ represents the amplitude of a harmonic function and the subscript 1 signifies approximate solutions for the acoustic pressure and velocity, which are solutions of the classical acoustic problem governed by the following equations and boundary conditions:

$$\frac{d^2 \hat{p}_1}{dx} + k_1^2 \hat{p}_1 = 0 \tag{16}$$

$$\rho_0 \frac{\partial u_1}{\partial t} + \frac{\partial p_1}{\partial x} = 0 \tag{17}$$

$$\frac{d\hat{p}_1}{dx} = 0 \quad (x = 0, L) \tag{18}$$

Comparison of Eqs. (14) and (15) reveals that the term

$$\left\langle [\, \rho_0 u_0 u_1^2]_0^L \right\rangle_{t,y}$$

appears only in Eq. (14). This may be attributed to the application of the boundary conditions shown in Eq. (18) in the solution of Eq. (16). The boundary conditions force the approximate velocity amplitude to zero at x = 0 and x = L. In this case, the omitted term is negligible. The benefit of the acoustic stability equation given in Eq. (14) is that it is applicable to more general types of oscillations. The term associated with the flow turning loss is also present in Eq. (14); that is,

$$\text{FLOW TURNING LOSS} = \left\langle \frac{1}{H}\int_0^L \langle u_1^2 \rangle_y [\, m_{b0}]_0^H dx \right\rangle_t \tag{19}$$

Inspection of this term shows that it is negative if mass enters the system through the top or bottom boundary, implying that it tends to reduce α and, thus, stabilize the system. On the other hand, if mass exits the system through the top or bottom boundary the term is always positive, which increases α and destabilizes the system. Unfortunately, a one-dimensional analysis cannot provide insight into the details of the flow turning loss mechanisms.

This analysis has confirmed that the flow turning loss is a part of the one dimensional acoustic stability equation. A secondary result of this analysis was a confirmation of Van Moorhem's[5] conclusion that the flow turning term is not absent from a three dimensional analysis as proposed by Culick[6], but that the term can only be isolated as a single term upon averaging over the cross section the duct. As suggested by Baum[7], the flow turning term describes a combination of several processes that result when flow is injected transverse to the acoustic motions. The inability to isolate a flow turning term in a three-dimensional analysis suggests that developing an understanding of the details of the mechanism that controls the flow turning loss may be very difficult.

Formulation for the Experimental Study

The one dimensional stability equation shown as Eq. (14) was derived by expanding the solutions in terms of first and second order quantities. While such a procedure is theoretically sound, it is hard to correlate first and order quantities with measured experimental data. Therefore, a new theoretical formulation that can be used in the experimental determination of the flow turning loss has been developed and it is presented in

this section. Starting with the following forms of the mass continuity and axial momentum equations

$$\frac{\partial \rho}{\partial t}+\frac{\partial}{\partial x}(\rho u)+\frac{\partial}{\partial y}(\rho v)=0 \tag{20}$$

$$\rho\frac{\partial u}{\partial t}+\rho u\frac{\partial u}{\partial x}+\rho v\frac{\partial v}{\partial y}+\frac{\partial p}{\partial x}=0 \tag{21}$$

and expressing each dependent variable as a sum of a time averaged component and a fluctuating component one obtains

$$\frac{\partial \bar{p}'}{\partial t}+\frac{\partial}{\partial x}\left(\bar{\rho}\bar{u}+\bar{\rho}u'+\rho'\bar{u}+\rho'u'\right)$$

$$+\frac{\partial}{\partial y}\left(\bar{\rho}\bar{v}+\bar{\rho}v'+\rho'\bar{v}+\rho'v'\right)=0 \tag{22}$$

$$\bar{\rho}\frac{\partial u'}{\partial t}+\left(\bar{\rho}+\rho'\right)\left[\bar{u}\frac{\partial \bar{u}}{\partial x}+\frac{\partial}{\partial x}\left(\bar{u}+u'\right)+u'\frac{\partial u'}{\partial x}\right]$$

$$+\left(\bar{\rho}+\rho'\right)\left[\bar{v}\frac{\partial \bar{u}}{\partial y}+\bar{v}\frac{\partial u'}{\partial y}+v'\frac{\partial \bar{u}}{\partial y}+v'\frac{\partial u'}{\partial y}\right]$$

$$+\frac{\partial \bar{p}'}{\partial x}=0 \tag{23}$$

where the bar and a prime denote a time averaged and a fluctuating quantity, respectively. Neglecting products of perturbations (which will be shown to be equivalent to neglecting terms of third order or higher in the result) and subtracting the time-invariant forms of the equations, Eqs. (22) and (23) become

$$\frac{\partial \bar{p}'}{\partial t}+\frac{\partial}{\partial x}\left(\bar{\rho}u'+\rho'\bar{u}\right)+\frac{\partial}{\partial y}\left(\bar{\rho}v'+\rho'\bar{v}\right)=0 \tag{24}$$

$$\bar{\rho}\frac{\partial u'}{\partial t}+\bar{\rho}\frac{\partial}{\partial x}\left(\bar{u}u'\right)+\rho'\bar{u}\frac{\partial \bar{u}}{\partial x}+\bar{\rho}\bar{v}\frac{\partial u'}{\partial y}$$

$$+\bar{\rho}v'\frac{\partial \bar{u}}{\partial y}+\rho'\bar{v}\frac{\partial \bar{u}}{\partial y}+\frac{\partial \bar{p}'}{\partial x}=0 \tag{25}$$

Assuming that the flow is isentropic, as was done in the previous analysis, multiplying Eqs. (24) and (25) by $\left(\frac{\bar{p}'}{\bar{\rho}}+\bar{u}u'\right)$ and $\left(\frac{\bar{\rho}'}{\bar{\rho}}\bar{u}+u'\right)$, respectively, adding the resulting equations, and averaging the resulting equation across the duct (i.e., y) one obtains:

$$\left\langle \frac{\partial}{\partial t}\int_0^L\left(\frac{\bar{p}'^2}{2\bar{\rho}\bar{a}^2}+\frac{\bar{\rho}\bar{u}^2}{2}+\frac{\bar{p}'\bar{u}u'}{\bar{a}^2}\right)dx\right\rangle_t$$

$$=-\left\langle\left[\bar{p}'u'+\frac{\bar{p}'^2\bar{u}}{\bar{\rho}\bar{a}^2}+\bar{\rho}\bar{u}u'^2\right]_0^L\right\rangle_{t,y}$$

$$-\left\langle\frac{1}{H}\int_0^L\left(\langle\bar{p}'\rangle_y\left[\bar{v}'\right]_0^H+\left\langle\frac{\bar{p}'}{\bar{\rho}\bar{a}^2}\right\rangle_y\left[\bar{v}\bar{p}'\right]_0^H\right)dx\right\rangle_t$$

$$-\left\langle\frac{1}{H}\int_0^L\left(\langle\bar{\rho}u'\rangle_y\left[\bar{v}'\bar{u}\right]_0^H\right)dx\right\rangle_t$$

$$+\left\langle\frac{1}{H}\int_0^L\left(\langle\bar{\rho}u'\rangle_y\left[\bar{v}u'\right]_0^H+\langle\bar{\rho}u'^2\rangle_y\left[\bar{v}\right]_0^H\right)dx\right\rangle_t \tag{26}$$

Using the relationship given in Eq. (13), Eq. (26) can be used to obtain the following expression for the complex growth rate constant of the oscillations,

$$2\alpha E_m^2=-\left\langle\left[\bar{p}'u'+\frac{\bar{p}'^2\bar{u}}{\bar{\rho}\bar{a}^2}+\bar{\rho}\bar{u}u'^2\right]_0^L\right\rangle_{t,y}$$

$$-\left\langle\frac{1}{H}\int_0^L\left(\langle\bar{p}'\rangle_y\left[\frac{\bar{m}'_b}{\bar{\rho}}\right]_0^H+\langle u'\rangle_y\left[\bar{m}'_b\bar{u}\right]_0^H\right)dx\right\rangle_t$$

$$-\left\langle\frac{1}{H}\int_0^L\left(\langle u'\rangle_y\left[\bar{m}_b u'\right]_0^H-\langle u^2\rangle_y\left[\bar{m}_b\right]_0^H\right)dx\right\rangle_t \tag{27}$$

where

$$E_m^2=\left\langle\int_0^L\left(\frac{\bar{p}'^2}{2\bar{\rho}\bar{a}^2}+\frac{\bar{\rho}u'^2}{2}+\frac{\bar{p}'\bar{u}u'}{\bar{a}^2}\right)dx\right\rangle_t \tag{28}$$

Comparison of Eqs. (14) and (27) reveals that the form of the equations is identical. However, it must be noted that the quantities involved in these equations are defined differently, and therefore the equations are not the same. Because of the way the terms have been defined, Eq. (27) lends itself more readily to the experimental verification of the flow turning losses.

Numerical Simulation

In order to determine the behavior and relative orders of magnitude of the various terms that appear in the developed stability expression, Eq. (27), a numerical simulation of the experimental setup that will be used to study the flow turning loss (see Fig. (1)) was carried out. The simulation involved derivation and numerical solution of the perturbed mass and axial momentum conservation equations for the proposed experimental setup; that is,

$$\left\langle \frac{\partial p'}{\partial t} \right\rangle_y + \left\langle \frac{\partial}{\partial x}\left(\bar{\rho}\,\overline{u'} + \overline{\rho' u'}\right) \right\rangle_y = -\frac{1}{H}\left[\bar{\rho}\,\overline{v'} + \overline{\rho' v'}\right]_0^H \qquad (29)$$

and

$$\left\langle \bar{\rho}\frac{\partial u'}{\partial t} \right\rangle_y + \left\langle \bar{\rho}\frac{\partial}{\partial x}\left(\bar{u}\,\overline{u'}\right) \right\rangle_y + \bar{\rho}\left\langle \bar{v}\frac{\partial u'}{\partial y} \right\rangle_y$$

$$+\bar{\rho}\left\langle v'\frac{\partial \bar{u}}{\partial y} \right\rangle_y + \left\langle \frac{\partial p}{\partial x} \right\rangle_y = 0 \qquad (30)$$

Equations (29) and (30) were derived assuming that 1) the flow is isentropic, 2) the perturbations are harmonic in time, 3) the y-dependence of the dependent variables is known, and 4) the pressure at the upstream injector plane is known (i.e., measured).

The derived mass and momentum conservation equations were then integrated along the axis of the experimental setup and their solutions substituted into the developed acoustic stability equation, Eq. (27), to determine the relative orders of magnitude of the various terms that appear in the equation and whether the numerical solutions satisfy Eq. (27). Since the solutions simulate the behavior of a "forced" experiment, the amplitude of the oscillations don't increase with time and the growth rate α must be zero. These calculations were carried out for a number of different experimental configurations and operating conditions, and in all cases excellent agreement between the results of the numerical simulation and the developed stability equation was obtained.

Results of a typical simulation are shown in Figs. (3) and (4). In order to simplify the calculations, the admittances of the upstream injector wall and burner surface were assumed to be to zero. Furthermore, it was assumed that the amplitude of the pressure oscillation at the injector face is 200 Pa, the mean pressure is atmospheric, the burner is 10 cm long and is located 70 cm downstream of the head end, and that the mean Mach number of the injected flow at the burner surface is 0.004, which simulates the Mach number of the flow at the multi-diffusion flame burner surface in a cold flow experiment. Figure (3) describes the axial variations of the amplitude and phase of the acoustic pressure along the experimental setup. The location of the burner is shown on the axis. It is seen that for the investigated Mach number, the effect of mass addition at the burner surface upon the pressure is small. The axial variations of the magnitudes of the various terms that appear in Eq. (27) are described in Fig. (4). The sum of these terms, which equals α, is also presented and it equals zero at all locations, in agreement with the theory. It should be noted, however, that the calculated magnitude of the flow turning loss for the experimental setup reveals that it is quite small. This is a consequence of the low injection Mach number and the small perturbation amplitude (compared to those experienced in unstable solid rocket motors), and does not suggest that the flow turning loss is always small. Figure (4) also shows that all the terms that are first order in Mach number are of similar magnitude. Because these terms are of similar order, Chen's[2] experimental approach, which did not account for all relevant terms in the stability equation, could not effectively measure the flow turning loss.

The numerical simulation was used to study the effects of several parameters upon the magnitude of the flow turning loss. One of these parameters was the location of the burner relative to the standing acoustic wave. The results of this study are presented in Fig. (5). It indicates that the flow turning loss depends upon where the injection occurs relative to the standing acoustic wave. The flow turning loss is maximum and minimum when the flow is injected near an acoustic velocity maximum and minimum, respectively. The second parameter studied was the mean core flow Mach number, which was varied from M = 0.0 to M = 0.1. This series of simulations showed that the magnitude of the flow turning loss was independent of the core velocity over the investigated range. Third, it was demonstrated that the flow turning loss varies linearly with the injection Mach number over an investigated range of M = 0.0 to M = 0.1. Finally, the dependence of the flow turning loss upon the amplitude of the acoustic pressure

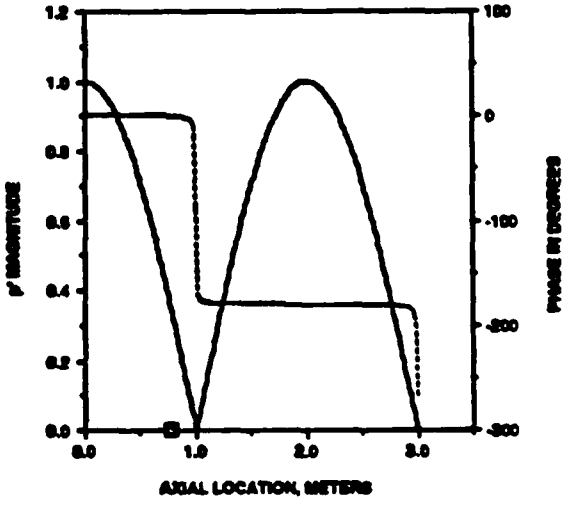

SOLID LINE - NORMALIZED AMPLITUDE OF p'
BROKEN LINE - PHASE OF ACOUSTIC PRESSURE p'

Figure 3. Numerically predicted amplitude and phase of the pressure oscillation in a duct with side injection near a pressure minimum. The phase is measured with respect to the pressure signal at x = 0. The injection occurs between x = 0.7 and x = 0.8.

oscillation was investigated and it was found that it is proportional to the square of the amplitude, as expected. Note, however, that the growth rate α is proportional to the loss of energy divided by the total energy, and so α is independent of the amplitude of the oscillations.

Concluding Remarks

The inclusion of flow turning losses in codes that predict the stability of solid rocket motors has been the subject of some controversy. The theoretical analysis performed in this paper has verified the existence of the term and, therefore, aids in validating its inclusion in one-dimensional stability predictions models. Furthermore, this study confirmed Van Moorhem's[3] conclusion that the one dimensional analysis contains no information that is not present in properly performed, three dimensional stability analyses. The flow turning term cannot, however, be isolated as a single term in the three dimensional analysis, suggesting that the term is due to an artificial grouping of terms, and not a single mechanism. This result clearly establishes that the mechanisms involved in the 'flow turning' term are already accounted for in a multi-dimensional analysis, and the addition of the term to a multi-dimensional analysis is not justified. For this reason, the study of the flow turning loss as it is currently understood must be restricted to a one-dimensional analysis.

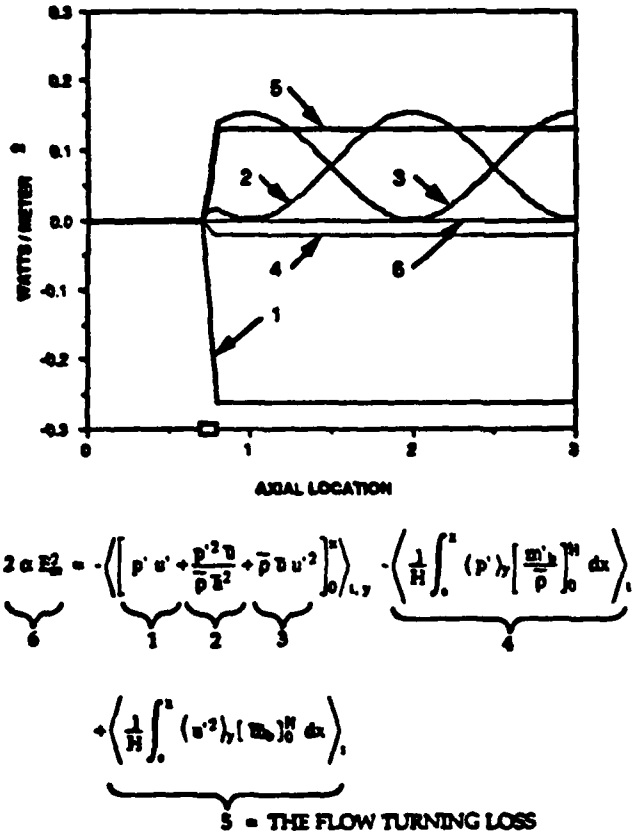

Figure 4. Numerical prediction of the relevant terms on the right hand side of the 1-dimensional acoustic stability equation for a duct with side injection from .7 to .8 meters from the head end, in this case near a pressure minimum.

The second result of this theoretical analysis was the development of an acoustic stability equation that can be used to experimentally determine the flow turning loss. The standard theoretical approach in which solutions are expanded in power series of the amplitude and Mach number does not produce results that can be readily used in the interpretation of experimental data because of the vague connection between the theoretical and measured variables. To resolve this problem, a different theoretical approach in which the dependent variables are written as the sum of a time-averaged and a fluctuating component, which can be measured, was developed. This model together with a simple numerical simulation of the proposed experimental set-up were then used to study the expected behavior of the experimental setup and relative orders of magnitude of the various terms in the derived stability equation. This analysis was carried out for a number of different experimental configurations and operating conditions, and in all cases excellent agreement between the results of the numerical simulation and the developed stability equation was obtained.

The next phase in this study is the experimental investigation of the flow turning loss using the newly developed stability equation. Measurements will be performed to determine the validity of the one-dimensional stability equation. The study will include experimental determination of the effects of various parameters, such as the location of the 'flow turning' region relative to the standing acoustic wave, the frequency and amplitude of the oscillation, and the magnitudes of the core flow and the injection velocities, upon the magnitude of the flow turning loss. These results will be then compared with analytical and numerical results.

References

1. Culick, F. E. C., "The Stability of One-Dimensional Motions in a Rocket Motor", *Combustion Science and Technology*, Vol. 7, 1973, pp. 165 - 175.
2. Chen, T., "Driving of Axial Acoustic Fields by Sidewall Stabilized Diffusion Flames," Ph.D. Thesis, Georgia Institute of Technology, July 1990.
3. Hersch, a. s. and Tso, J., "Flow-Turning Losses in Solid Rocket Motors," Final Report, Air Force Astronautics Laboratory Grant No. AFAL-TR-87-095, March 1988.
4. Cantrell, R. H. and Hart, R. W., "Interactions Between Sound and Flow in Acoustic Cavities: Mass, Momentum, and Energy Considerations," *Journal of the Acoustical Society of America*, Vol. 36, No. 4, April 1964.
5. Van Moorhem, W. K., "Theoretical Basis of the Flow Turning Effect in Combustion Stability," Final Report, AFOSR Grant No. AFOSR-78-3645, March 1980.
6. Culick, F. E. C., "Stability of Three-Dimensional Motions in a Combustion Chamber," *Combustion Science and Technology*, Vol. 10, 1775, pp. 109 - 124.
7. Baum, J. D., "Investigation of Flow Turning Phenomenon; Effects of Frequency and Blowing Rate," AIAA Paper No. AIAA-89-0297, Presented at the 27th Aerospace Sciences Meeting, Jan. 9-12, 1989, Reno, Nevada.

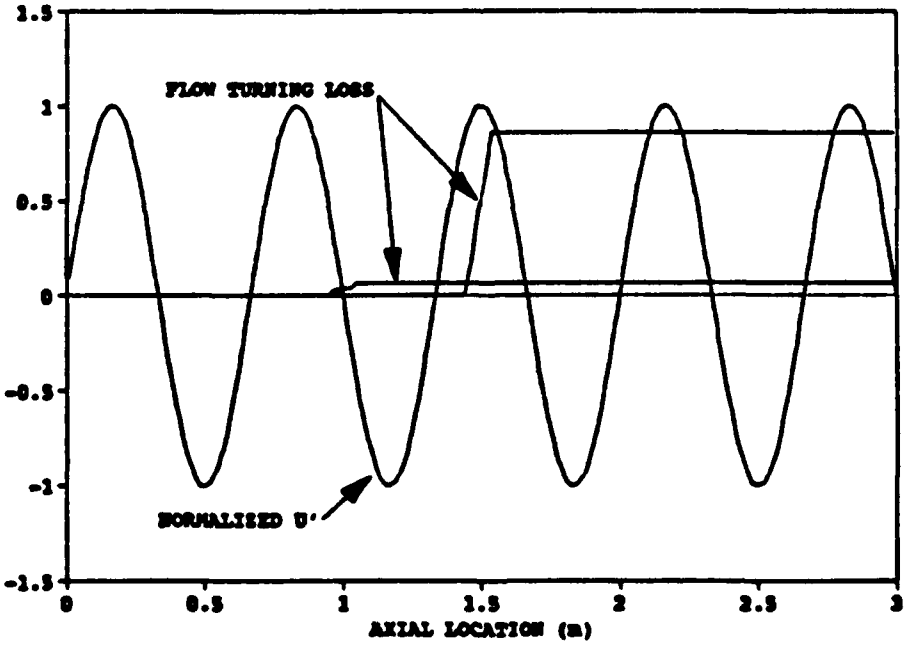

Figure 5. Numerically predicted flow turning loss for injection at an acoustic velocity minimum and at an acoustic velocity maximum showing the dependence of the term upon the injection location. Normalized acoustic velocity is shown for reference.

AIAA 93-0115

Investigation of Flow Turning Loss in a Simulated Unstable Solid Propellant Rocket Motor

L. M. Matta and B. T. Zinn
Georgia Institute of Technology
Atlanta, GA

31st Aerospace Sciences
Meeting & Exhibit
January 11-14, 1993 / Reno, NV

INVESTIGATION OF FLOW TURNING LOSS IN A SIMULATED UNSTABLE SOLID PROPELLANT ROCKET MOTOR*

L. M. Matta and B. T. Zinn**
School of Aerospace Engineering
Georgia Institute of Technology

ABSTRACT

This paper describes an experimental investigation of the flow turning loss in unstable solid propellant rocket motors. It is caused by the interaction of the radially directed flow of combustion products leaving the propellant surface with the axial acoustic field. The experimental setup consisted of a rectangular duct with side injection that simulated the combustion products leaving the propellant surface. Acoustic drivers were used to excite oscillations that simulated an axial instability. The mean and acoustic velocities and the acoustic pressure oscillations were measured in a region where the flow turning loss was expected to occur. The measured data were used to evaluate the terms that appear in an acoustic stability equation containing the various loss and gain terms including the flow turning loss. Experiments were performed to determine the effects of the injection and mean flow Mach numbers, the amplitude of the oscillation and the location of the burner relative to the standing wave upon the magnitude of the flow turning loss in the investigated control volume. The flow turning loss was shown to depend strongly upon the injection velocity and the location of the injection relative to the standing wave. Measured data compared well with numerical predictions.

INTRODUCTION

The objective of this investigation is to develop a better understanding of the flow turning loss and other processes that contribute to the driving and damping of axial instabilities in solid propellant rocket motors. This understanding is necessary for the development of practical methods for the design of stable solid propellant rocket motors.

The occurrence of combustion instability is determined by the relative magnitudes of the various driving and damping mechanisms within the rocket motor that add and remove energy from the oscillations, respectively. If the acoustic energy gains outweigh the losses, small perturbations amplify to levels that can adversely affect guidance, thrust history, and the structural integrity of the motor[1-4]. In order to eliminate or reduce the severity of acoustic oscillations resulting from combustion instabilities in solid rocket motors, the mechanisms by which energy is added to and removed from these oscillations must be identified and understood. It is generally accepted that the interaction between the solid propellent combustion process and the acoustic oscillations provides the energy necessary to initiate and maintain instabilities in rocket motors. Other factors, such as nozzle damping, viscous dissipation, and flow turning generally remove energy from the oscillations and thus stabilize the system.

The velocity of combustion products is generally radial at the burning solid propellant surface. As these gasses move away from the propellant and are entrained in the core flow, they are turned from radial to axial, as shown in Fig. 1. During this turning process, the combustion products that leave the burning propellant surface with no axial acoustic momentum must acquire axial acoustic energy from the core flow oscillations. This phenomena was first discussed by Culick[5] who argued that since the combustion products entering the core flow acquire acoustic energy from the axial acoustic field (i.e., the core flow oscillations), the axial acoustic field loses acoustic energy, which tends to stabilize the system.

The flow turning phenomenon has been studied experimentally by Hersch[6,7] and Chen[8] and analytically by Baum[9,10] and Hegde[11-13]. In these investigations, the behavior of acoustic waves in a channel in which the solid propellant combustion process was simulated by mass addition through a side wall was investigated. Hersch's conclusions were inconsistent with the behavior of the flow turning loss as predicted by Culick. Also, the accuracy of the results of both Hersch's and

* Research supported under AFOSR Contract No. 91-0160; Dr. M. A. Birkan contract monitor.
** Regents Professor, Aerospace Engineering, Fellow AIAA

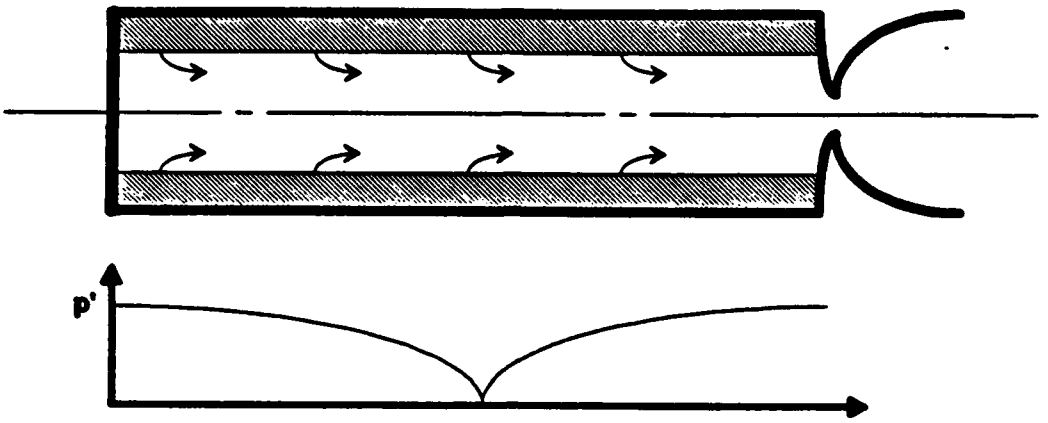

Figure 1. Schematic of a solid propellant rocket motor showing the flow of combustion products turning from radial to axial as they are entrained into the core flow and the pressure distribution characteristic of axial acoustic instability.

Chen's investigations are open to question due to the methods employed. Baum's[9,10] computational studies show that the flowfield near the wall is extremely complex, involving a multitude of vortical structures and energy exchange between the mean flow and the oscillations. Hegde et al[11-13] used a linear analysis and hot wire measurements to determine the acoustic characteristics and losses of a duct containing a standing axial acoustic wave and mass addition through the side wall. His results, in contrast with those of Baum, suggest that a linear model may be adequate for describing the important features of the flow field in an unstable solid propellant motor.

The goal of this project is to determine the validity of the flow turning loss term that is included in currently used one dimensional linear stability prediction codes. The first step was to verify the existence and mathematical form of the flow turning loss as defined by Culick[5]. To this end, a one-dimensional acoustic stability equation was derived using an energy balance approach similar to that used by Cantrell and Hart[14] with the addition of flow rotation effects. This analysis confirmed that the classical flow turning loss term is indeed a part of the one dimensional acoustic stability equation. This analysis also confirmed Van Moorhem's[15] conclusion that the flow turning loss is not absent from three dimensional stability models as suggested by Culick[16]. It was shown that the "classical" flow turning loss term results from the cross sectional averaging used to reduce the three dimensional problem to one dimension. The inability to isolate the flow turning term in a three dimensional stability equation suggests that developing an understanding of the details of the mechanisms involved in the term may be impossible.

The second phase of this program focused on the development of an acoustic stability equation that was better suited to the interpretation of experimental data. The one dimensional acoustic stability equation is ordinarily derived by expanding the governing equations in terms of first and second order quantities. While such a procedure is theoretically sound, it is difficult to correlate first and second order quantities with measured data. Therefore, a new theoretical approach was developed which simplifies the interpretation of data in the experimental determination of the flow turning loss. This approach begins from the equations of mass and axial momentum conservation in which each of the dependent variables is expressed in terms of a time averaged and a fluctuating component. For example, the pressure is expressed as

$$p = \overline{p} + p' \qquad (1.1)$$

where $\overline{p}$ is the time average of the measured pressure. The procedure is explained more thoroughly in Ref. 17.

The equation for the growth rate constant derived by this method for a 2-D rectangular volume of length L and height H is

$$2\alpha E^2 = -\left\langle \left[p'u' + \frac{p'^2\bar{u}}{\bar{\rho}\bar{a}^2} + \bar{\rho}\bar{u}u'^2 \right]_0^L \right\rangle_{t,y}$$

$$-\left\langle \frac{1}{H}\int_0^L \left(\langle p' \rangle_y \left[\frac{m_b'}{\bar{\rho}} \right]_0^H \right) dx \right\rangle_t$$

$$-\left\langle \frac{1}{H}\int_0^L \left(\langle u' \rangle_y [m_b'\bar{u}]_0^H + \langle u' \rangle_y [\bar{m}_b u']_0^H \right) dx \right\rangle_t$$

$$+\left\langle \frac{1}{H}\int_0^L \left(\langle u'^2 \rangle_y [\bar{m}_b]_0^H \right) dx \right\rangle_t \qquad (1.2)$$

where α is the acoustic growth rate constant, E^2 is a term with units of energy, u and v represent the axial and transverse velocity components, respectively, and m_b is the mass flux at the wall. The terms in this equation were grouped in a way that permits comparison with Culick's result. As noted by Culick[5], the proper choice of groupings is not obvious, as spatial averaging of terms makes it difficult to physically interpret these terms. The term in Eq. 1 that describes the flow turning loss is given by

FLOW TURNING LOSS =

$$\left\langle \frac{1}{H}\int_0^L \left(\langle u'^2 \rangle_y [\bar{m}_b]_0^H \right) dx \right\rangle_t \qquad (1.3)$$

Inspection of this term shows that it will always be negative in a rocket motor where mass enters through the burning surfaces. For such a configuration this term tends to reduce α, which stabilizes the system. On the other hand, if mass exits the system through a side wall (e.g., as through a T-burner nozzle), this term is positive, which increases α and destabilizes the system.

EXPERIMENTAL STUDY

The experimental study was conducted in the setup shown in Fig. 2. It was designed to simulate flow phenomena near the walls of a solid propellant rocket experiencing an axial acoustic instability. The facility consists of a duct 7.6 cm (3.0 in.) high by 3.8 cm (1.5 in.) wide by 3 m (9.1 ft.) long steel duct with a flat flame burner mounted on the bottom wall. The multi-diffusion flame burner, which was designed to simulate a gas phase solid propellant flame, consists of a matrix of hypodermic tubes which supply oxidizer flow, simulating the flow of combustion products from burning ammonium perchlorate particles. Fuel is supplied through the spaces between the tubes, which simulates the flow of pyrolysis products from the fuel binder. In cold flow experiments, room temperature air is injected through the burner. To date, only cold flow experiments have been performed. Two acoustic drivers mounted on opposing duct walls just upstream of the exit plane are used to excite a standing acoustic wave in the duct that simulates an axial instability in a rocket motor. Axial core flow is simulated by the injection of air at the upstream end of the duct through a movable porous plate injector. The location of the wall mounted burner (and, therefore, the flow turning

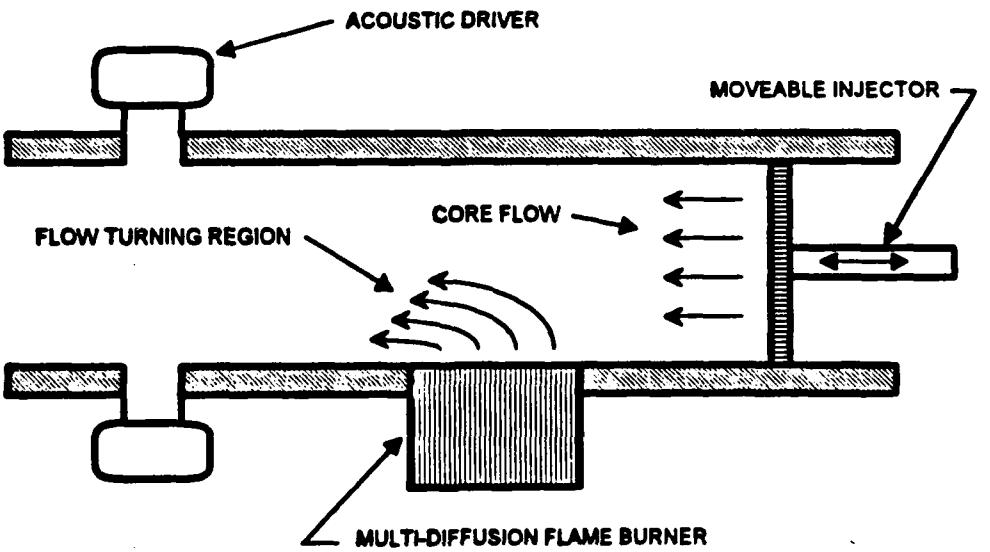

Figure 2. Schematic of the experimental setup used in the flow turning studies.

region) relative to the standing acoustic wave can be varied by axial translation of the core flow injector. Velocity measurements were performed using an LDV system through quartz windows in the side walls adjacent to the wall mounted burner. Acoustic pressures were measured with a 1/4 in. Brüel & Kjær microphone probe.

In a typical experiment, the components of the mean and acoustic velocities and the acoustic pressure were measured on a rectangular grid in the region above the burner where flow turning loss was expected to occur. A typical mean velocity field is shown in Fig. 3. In this configuration the core flow was injected from the right, the burner was on the bottom, and the acoustic drivers were located downstream (to the left) of the displayed control volume. The acoustic intensity vector field for this configuration, shown in Fig.4, reveals that for these test conditions (i.e., frequency, core flow velocity, burner injection velocity, and position of injection point with respect to the standing axial acoustic wave) a relatively large amount of the acoustic energy is directed into the burner where it is most likely absorbed. This turning of the acoustic intensity flow represents a zeroth order (in Mach number) acoustic energy loss. The amount of acoustic

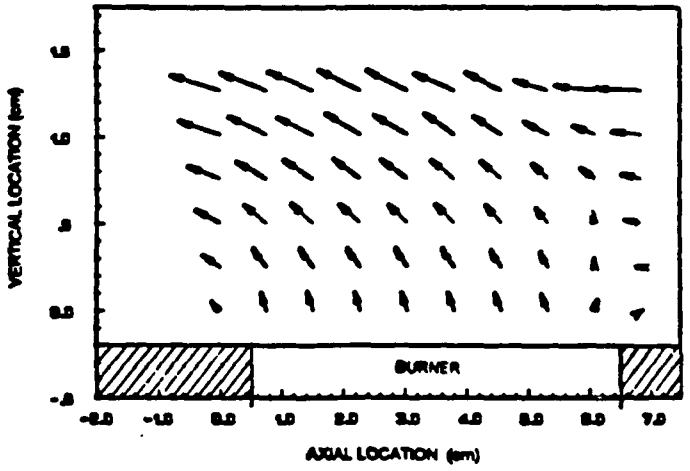

Figure 3. Vector plot of a typical measured mean velocity field in the flow turning region.

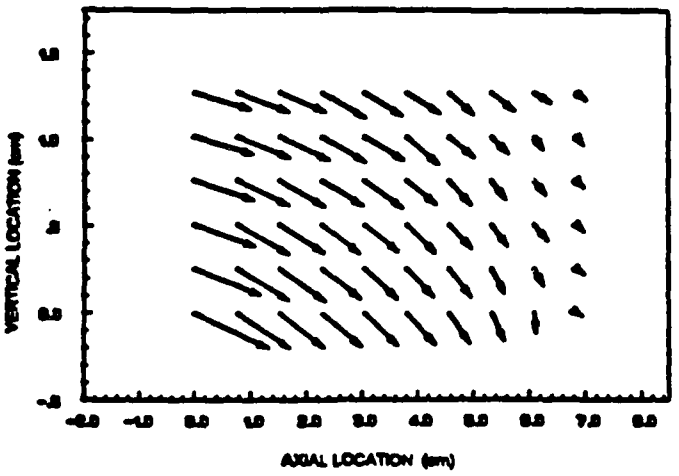

Figure 4. Diagram of typical measured acoustic intensity, $< p' U' >$.

intensity absorbed by the burner depends upon the test condition.

The results of two series of tests are presented in Figs. 5 and 6. Figure 5 describes the results of a study of the dependence of the flow turning loss upon the mean core flow Mach number M_c. These data were obtained by varying the mean flow rate injected through the porous injector at the entrance of the duct. Theoretical analysis and numerical predictions indicate that the flow turning loss does not depend upon M_c, which contradicts the experimental results. This discrepancy results from the fact that the numerical and theoretical studies investigated the behavior of a control volume that spanned the entire cross section of the duct, forcing all the injected flow to turn in the direction of the axis. In contrast, the experimental study investigated the flow behavior within a control volume that did not extend from the burner surface to the top wall. Consequently, as shown in Fig. 3, the flow at the top of the control volume is not "fully turned" into the axial direction. As the core flow Mach number increases, the amount by which the flow injected through the wall mounted burner is turned also increases. Therefore, it is expected that as the core flow Mach number increases, the measured flow turning loss will also increase, which is consistent with the trend exhibited by the data presented in Fig. 5.

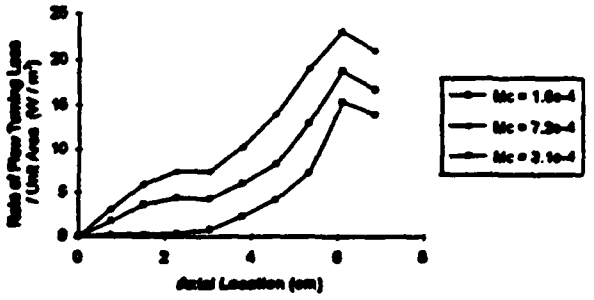

Figure 5. Axial variation of the flow turning loss for 3 core flow Mach numbers.

The results of a study of the dependence of the flow turning loss upon the burner injection Mach number M_b are presented in Fig. 6. In this case, the flow turning loss is plotted for three tests in which only the rate of mass injection was varied. The theoretical predictions indicate a linear relationship between the burner injection Mach number and the magnitude of the flow turning loss. While the experimental results clearly show that the flow turning loss increases with

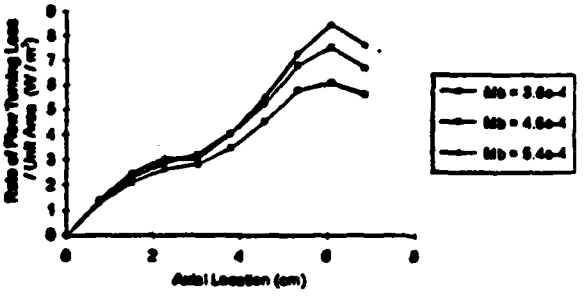

Figure 6. Axial variation of the flow turning loss term for 3 burner injection Mach numbers.

M_b, this relationship is not linear. The discrepancy is again believed to be due to the incomplete flow turning in the investigated control volume. As M_b increases, the flow turning region thickens and the flow turning process requires a larger region above the burner for completion. It is expected, therefor, that the rate at which the flow turning loss in the investigated control volume increases with M_b will be less than linear, and this agrees with the observed results.

The term α_{FTL} describes the contribution of the flow turning loss to the growth rate constant a of the investigated region. The effects of the investigated parameters upon α_{FTL} are shown in Figs. 7-13. Figures 7 and 8 show the effect of burner injection velocity upon α_{FTL} in the investigated region for two experiments. The results shown in Fig. 7 were obtained from the experimental setup configured as follows: the frequency of oscillation was 550 Hz., the mean core flow velocity was 0.4 m/s, and the injection occurred at a pressure node. The measured α_{FTL} varies linearly with the mean burner injection velocity. Figure 8

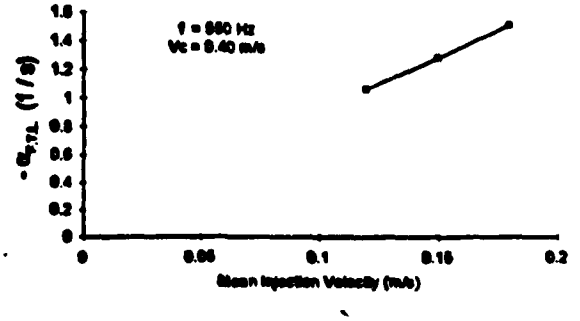

Figure 7. Dependence of α_{FTL} upon the mean burner injection Mach number.

shows results obtained with a mean core flow velocity of 1.77 m/s, a 550 Hz. oscillation, and the flow turning region located between a pressure node and antinode. The measured α_{TTL} is again observed to vary linearly with the burner injection velocity. This linear relationship agrees with the theoretical and numerical predictions.

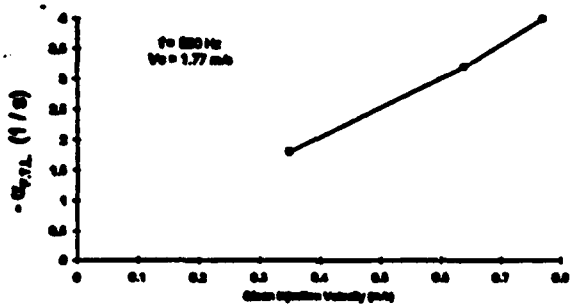

Figure 8. Dependence of α_{TTL} upon the mean burner injection Mach number.

Figures 9 and 10 show the dependence of α_{TTL} in the investigated region upon the mean core flow velocity; the data in Fig. 9 were measured in tests with a frequency of 550 Hz., a burner injection velocity of 0.156 m/s, and the burner located at a pressure node; the data in Fig. 10 were obtained with a frequency of 480 Hz., a burner injection velocity of 1.02 m/s and the flow turning region located between a pressure node and a pressure antinode. In both series of tests, the measured α_{TTL} increased with the mean core flow velocity and appears to approach a limit. Again, as discussed before, it is believed that this behavior is due to incomplete flow turning in the investigated region. Numerical simulations predict this behavior when this

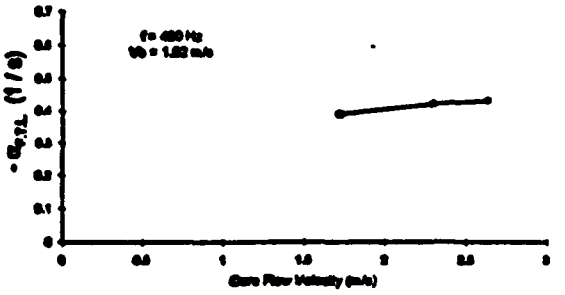

Figure 10. Dependence of α_{TTL} upon the mean core flow Mach number.

incomplete flow turning process is accounted for. It should be pointed out, however, that the difference in the trends exhibited by the data in Figs. 9 and 10 is due to the fact that in the tests described in Fig. 10 the magnitude of the core flow velocity was high enough that its effect upon the flow turning loss is small.

The dependence of α_{TTL} upon the amplitude of the excited acoustic wave is presented in Figs. 11 and 12. Figure 11 describes tests conducted with mean core flow velocity of 2.25 m/s, mean burner injection velocity of 0.76 m/s, 300 Hz. frequency, and injection between an acoustic pressure node and an antinode while Fig. 12 describes tests conducted with a mean core flow velocity of 1.45 m/s, mean burner injection velocity of 0.62 m/s, a 550 Hz. frequency, and injection at an acoustic pressure antinode. The pressure amplitudes were normalized with respect to the largest amplitude oscillation. Both figures show that α_{TTL} is independent of the amplitude of oscillation, which is

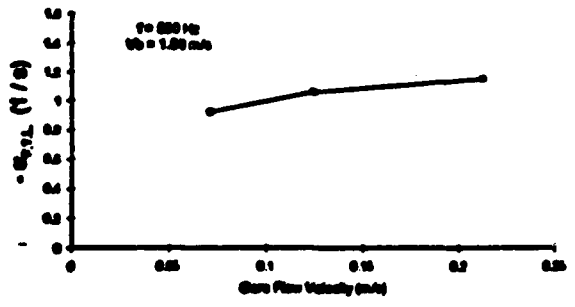

Figure 9. Dependence of α_{TTL} upon the mean core flow Mach number.

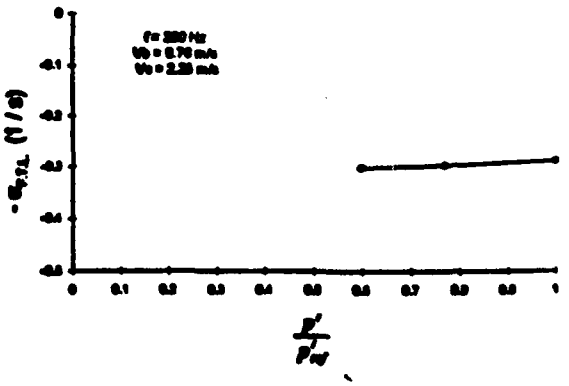

Figure 11. Dependence of α_{TTL} upon the non-dimensional amplitude of oscillation.

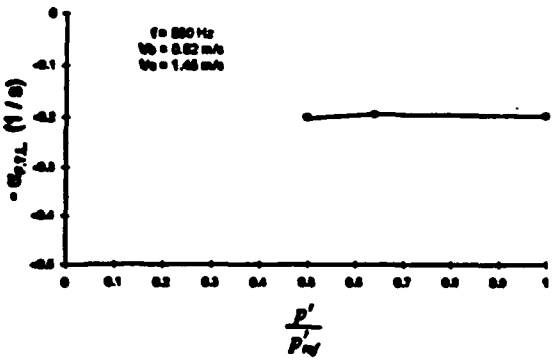

Figure 12. Dependence of α_{FTL} upon the non-dimensional amplitude of oscillation.

expected in a linear analysis and is in agreement with theory and calculations.

The dependence of the measured value of α_{FTL} upon the location of the flow turning region relative to the standing acoustic wave is shown in Fig. 13. This experiment was performed with a mean core velocity of 2.86 m/s, mean burner injection velocity of 1.34 m/s, and a frequency of 550 Hz. The measured α_{FTL} was greatest when the flow turning occurred at an acoustic pressure node, and the smallest when the flow turning region was located at a pressure antinode. This trend is in agreement with the theoretical prediction that a_{FTL} is proportional to u'^2.

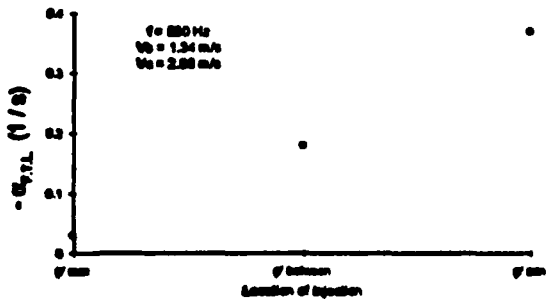

Figure 13. Dependence of α_{FTL} upon the location of the flow injection point relative to the standing acoustic wave.

A numerical simulation of the investigated experimental setup using measured boundary conditions was performed to determine whether the experimental results could be modelled. The simulation involved the derivation and numerical solution of the perturbed mass and axial momentum conservation equations for the developed experimental setup, assuming that the flow was isentropic and the perturbations were harmonic in time. The equations were integrated along the axis of the experimental setup and their solutions were used to determine the values of the various terms that appear in the acoustic stability equation. The results of a typical simulation are shown in Figs. 14-16. The cross-duct average of the measured axial acoustic velocity and the corresponding calculated values for a typical experimental configuration are shown in Fig. 14. The agreement between the measured and calculated velocities is excellent.

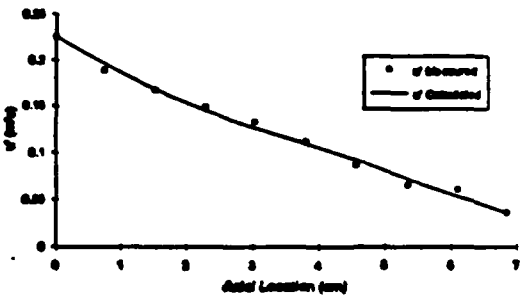

Figure 14. Comparison of measured and calculated values of the cross-sectional average of the axial acoustic velocity in the flow turning region.

Figure 15 presents comparisons between the measured and calculated acoustic pressure amplitudes and phases between the pressure and velocity oscillations. Good agreement between the calculated pressure and measured pressure amplitudes is observed, but the error between the calculated and measured phase values is large.

The calculated and measured values of the flow turning loss for this test configuration are shown in Fig. 16, which shows excellent agreement between the measured and calculated values. Note that the value of the flow turning loss term in this experiment is negative, indicating a gain of acoustic energy. This is observed because of the nature of the flow in the investigated control volume. The flow injected through the burner is turned into the axial direction, while simultaneously the core flow entering the control volume from upstream is being turned upward. For

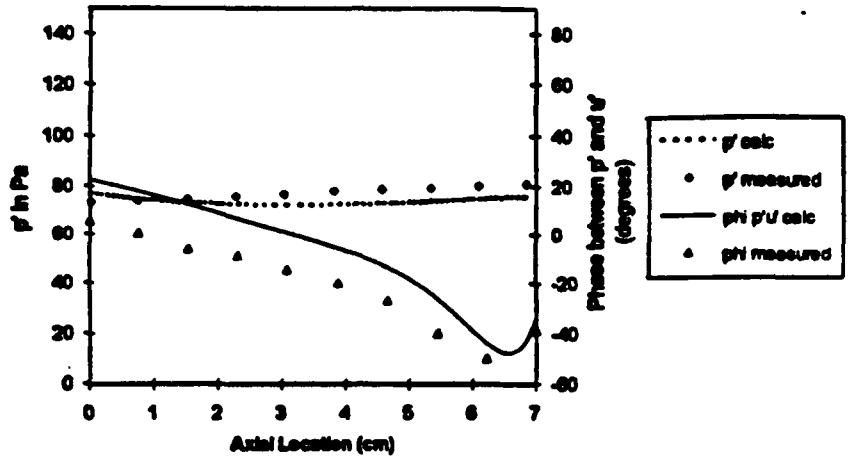

Figure 15. Comparisons between measured and calculated cross-sectional averages of the acoustic pressure amplitudes and phase angles between the pressure and the axial velocity oscillations in the flow turning region.

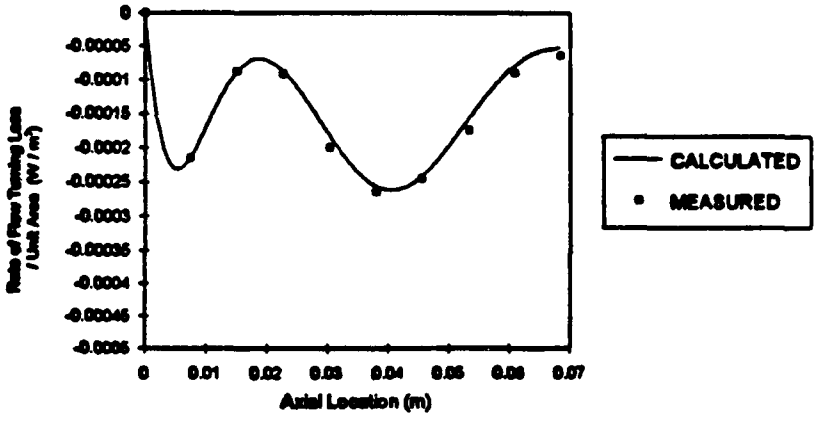

Figure 16. Comparison of measured and calculated values of the axial variations of the rate of flow turning loss across the investigated control volume.

some experimental configurations, the flow turning loss due to the turning of the injected flow is smaller than the "flow turning gain" due to the turning of the core flow. This flow turning gain effect is observed only because of the choice of control volumes; it will not occur in a volume extending from wall to wall where a flow turning loss will always occur.

CONCLUDING REMARKS

This paper reports the results of an experimental investigation of the flow turning loss in a setup designed to simulate a region near a burning propellant surface in a solid propellant motor experiencing an axial instability. The mean and acoustic velocities as well as the acoustic pressures were measured throughout a control volume encompassing the flow turning region, and the measured data were used to evaluate the flow turning loss and related terms in an acoustic stability equation developed earlier under this program. These measurements showed that the magnitude of the flow turning loss is mainly determined by the wall injection velocity and the location of the injection point relative to the standing acoustic wave.

This conclusion agrees with the predictions of existing theoretical models.

Measured boundary conditions were used in a previously developed numerical simulation of the experimental setup. The calculated values of the cross-section average of the axial acoustic velocity, acoustic pressure amplitude, the phase between the axial velocity and pressure, and the axial variation of the flow turning term were compared to measured values. The inviscid equations used in the numerical simulation were able to adequately predict the magnitudes of the pressure and axial velocity variations (and, therefore, the flow turning loss term), but did not accurately predict the phase between them. This failure to predict the zeroth order (in Mach number) acoustic energy loss suggests the possibility that viscous driving or damping mechanisms that are not treated in this analysis or accounted for in standard stability prediction methods, may be important. In order to investigate this possibility, detailed numerical modelling of the experimental setup using a full Navier-Stokes solver is currently underway. Results from the study will be used in conjunction with previous results to determine the importance of the viscous terms in axial stability predictions.

REFERENCES

1) McClure, F. T., Hart, R. W., and Cantrell, R. H., "Interaction Between Sound and Flow: Stability of T-Burners," *AIAA Journal*, Vol. 1, No. 3, March 1963.

2) Derr, R. L., Mathes, H. B., and Crump, J. E., "Application of Combustion Instability Research to Solid Rocket Motor Problems," 53rd Meeting of the NATO AGARD Propulsion and Energetics Panel, Oslo, Norway, April 2-5, 1979.

3) Baum, J. D., "Acoustic Energy Exchange Through Flow Turning," AIAA Paper No. 87-0217, presented at the 25th Aerospace Sciences Meeting, Jan. 12-15, 1987, Reno, NV.

4) Sutton, G. P., Rocket Propulsion Elements, 5th Ed., pp. 310-312, John Wiley and Sons, Inc., 1986.

5) Culick, F. E. C., "The Stability of One Dimensional Motions in a Rocket Motor", *Combustion Science and Technology*, Vol. 7, 1973, pp. 165-175.

6) Hersch, A. S., and Walker, B., "Experimental Investigation of Rocket Motor Flow Turning Losses," AIAA Paper No. 83-1267, June 1983.

7) Hersch, A. S., and Tso, J., "Flow Turning Losses in Solid Rocket Motors," AFAL-TR-095, March 1988.

8) Chen, T., "Driving of Axial Acoustic Fields By Sidewall Stabilized Diffusion Flames," Ph.D. Thesis, Georgia Institute of Technology, July 1990.

9) Baum, J. D., and Levine, J. N., "Acoustic-Mean Flow Interaction," AFRPL-TR-86-065, January 1987.

10) Baum, J. D., "Numerical Investigation of Energy Exchange Mechanisms Between Mean and Acoustic Flow Fields in a Simulated Rocket Combustor," AIAA-90-2310, 26th Joint Propulsion Conference, Orlando, FL, 1990.

11) Hegde, U. G., Chen, F., and Zinn, B. T., "Investigation of the Acoustic Boundary Layer in Porous Walled Ducts With Flow," *AIAA Journal*, Vol. 24, No. 9, pp. 1474-1482, September 1986.

12) Hegde, U. G., and Zinn, B. T., "Rocket Motor Flow Turning Losses," *AIAA Journal*, Vol. 24, No. 8, pp. 1394-1396, August, 1986.

13) Hegde, U. G., and Zinn, B. T., "The Acoustic Boundary Layer in Porous Walled Ducts With a Reacting Flow," Proceedings of the Twenty-First Symposium on Combustion, August 1986.

14) Cantrell, R. H., and Hart, R. W., "Interactions Between Sound and Flow in Acoustic Cavities: Mass, Momentum, and Energy Considerations," *Journal of the Acoustic Society of America*, Vol. 36, No. 4, April 1964.

15) Van Moorhem, W. K., "Theoretical Basis of the Flow Turning Effect in Combustion Stability," Final Report, AFOSR Grant No. 78-3654, March 1980.

16) Culick, F. E. C., "Stability of Three-Dimensional Motions in a Combustion Chamber," *Combustion Science and Technology*, Vol. 10, 1975, pp. 109-124.

17) Matta, L. M., Zinn, B. T., and Daniel, B. R., "Theoretical Investigation of Flow Turning Losses in an Experimental Setup Which Simulates Instabilities in Solid Propellant Rocket Motors," AIAA paper no. 92-0780, presented at the 30th Aerospace Sciences Meeting, Reno NV, Jan. 6-9, 1992